Kinesin-related *KIP3* of *Saccharomyces cerevisiae* Is Required for a Distinct Step in Nuclear Migration

Todd M. DeZwaan,* Eric Ellingson,‡ David Pellman,‡ and David M. Roof*

*Department of Physiology, University of Pennsylvania School of Medicine, Philadelphia, Pennsylvania 19104-6085; and ‡Departments of Pediatric Oncology, The Dana-Farber Cancer Institute, and Pediatric Hematology, The Children's Hospital, Harvard Medical School, Boston, Massachusetts 02115

Abstract. Spindle orientation and nuclear migration are crucial events in cell growth and differentiation of many eukaryotes. Here we show that *KIP3,* the sixth and final kinesin-related gene in *Saccharomyces cerevisiae*, is required for migration of the nucleus to the bud site in preparation for mitosis. The position of the nucleus in the cell and the orientation of the mitotic spindle was examined by microscopy of fixed cells and by time-lapse microscopy of individual live cells. Mutations in *KIP3* and in the dynein heavy chain gene defined two distinct phases of nuclear migration: a *KIP3*-dependent movement of the nucleus toward the incipient bud site and a dynein-dependent translocation of the nucleus through the bud neck during anaphase. Loss of *KIP3* function disrupts the unidirectional movement of the nucleus toward the bud and mitotic spindle orientation, causing large oscillations in nuclear position. The oscillatory motions sometimes brought the nucleus in close proximity to the bud neck, possibly accounting for the viability of a *kip3* null mutant. The *kip3* null mutant exhibits normal translocation of the nucleus through the neck and normal spindle pole separation kinetics during anaphase. Simultaneous loss of *KIP3* and kinesin-related *KAR3* function, or of *KIP3* and dynein function, is lethal but does not block any additional detectable movement. This suggests that the lethality is due to the combination of sequential and possibly overlapping defects. Epitope-tagged Kip3p localizes to astral and central spindle microtubules and is also present throughout the cytoplasm and nucleus.

MICROTUBULES mediate a series of movements in *Saccharomyces cerevisiae* that culminate in chromosome segregation, including migration of the nucleus to the neck between the mother and daughter cells, assembly of a bipolar spindle, translocation of the spindle through the neck, and elongation of the spindle during anaphase. Movements have been associated with the action of particular microtubule-based motor proteins by examining mutants defective in motor function and identifying the perturbed movement. One complication in this approach is that a single movement may be generated by two or more motor proteins, as occurs in yeast cells during spindle pole separation (Hoyt et al., 1992; Roof et al., 1992). Disruption of a motor for a redundantly powered movement may fail to generate a terminal cell morphology that reveals all roles performed by the motor. However, *S. cerevisiae* has a modest set of cytoskeletal movements and motors, which has allowed significant progress to be made in associating particular movements with the activity of one or more motor proteins. One movement that has yet to be associated with a force-generating protein is migration of undivided nuclei to the neck of the emerging bud, which proceeds in all motor mutants examined to date.

The position of the nucleus and mitotic spindle within the cell is under complex control at all stages of the cell cycle. In budding cells, the preanaphase nucleus is typically located a short distance from the bud neck, and microtubules from one spindle pole pass through the neck and into the bud (Byers and Goetsch, 1975). Analysis of specific β-tubulin alleles has demonstrated that astral (or cytoplasmic) microtubules play a key role in nuclear and spindle positioning (Palmer et al., 1992; Sullivan and Huffaker, 1992). Microtubule-independent mechanisms also appear to affect the position of the nucleus. When cell cycle progression is arrested in metaphase after nuclear migration to the neck is complete, the nucleus is retained at the neck upon microtubule depolymerization (Jacobs et al., 1988). Furthermore, the actin cytoskeleton is thought to play a role because disruption of actin in cells arrested in metaphase causes the spindle to be improperly oriented with respect to the neck (Palmer et al., 1992).

Upon initiation of anaphase, the spindle is approximately aligned along the mother–daughter axis so that one

Address all correspondence to David M. Roof, Department of Physiology, University of Pennsylvania School of Medicine, Philadelphia, PA 19104-6085. Tel.: (215) 573-3636. Fax: (215) 573-5851. E-mail:roof@mail.med.upenn.edu

spindle pole inserts through the narrow opening of the bud neck, allowing spindle elongation to place the divided genomes at the distal edges of the mother and daughter cells. One motor protein that appears to exert force on the nucleus as anaphase commences is dynein. Mutants defective in the gene for dynein heavy chain (*dhc1* or *dyn1* mutants) fail to translocate the early anaphase nucleus through the neck, which causes the spindle to elongate within the mother cell and results in the formation of a binucleate cell (Eshel et al., 1993; Li et al., 1993; Yeh et al., 1995). Dynein mutants also fail to exhibit the back and forth movement of the anaphase spindle within the neck observed in wild-type cells, supporting a role for dynein in spindle positioning during anaphase (Yeh et al., 1995). Dynactin, a protein complex associated with dynein, also appears to be required for nuclear translocation because null alleles of the putative *S. cerevisiae* dynactin components *JNM1* and *ACT5* have an identical phenotype to dynein disruption mutants (McMillan and Tatchell, 1994; Muhua et al., 1994). Although dynein has a role in positioning the nucleus after the onset of anaphase, analysis of cells arrested in metaphase suggests that dynein is not required to position the nucleus at the bud neck (Yeh et al., 1995).

Dynein has also been implicated in generating forces for spindle pole separation during anaphase B, along with the kinesin-related proteins Kip1p and Cin8p (Saunders et al., 1995; Yeh et al., 1995). Kinetic analysis of spindle pole separation in live cells has shown that loss of dynein function slows the rate of spindle pole separation in late anaphase (Yeh et al., 1995). Analysis of populations of fixed cells has shown that loss of Kip1p and Cin8p function abolishes pole separation during spindle assembly and causes an inward collapse of metaphase spindle poles (Hoyt et al., 1992; Roof et al., 1992; Saunders and Hoyt, 1992). Simultaneous loss of dynein, Kip1p, and Cin8p function abolishes anaphase spindle elongation, while individual or pair-wise loss of function of these proteins had smaller effects (Saunders et al., 1995). Mutations in another kinesin-related motor, Kar3p, can suppress the spindle collapse caused by loss of Kip1p and Cin8p function. This suggests that Kar3p contributes to a force that opposes an outwardly directed force on the spindle poles generated by Kip1p and Cin8p (Hoyt et al., 1993). Nonmotor microtubule-associated proteins are also required for anaphase B (Pellman et al., 1995).

Given the cooperation between motor proteins in generating movements, a thorough understanding of the underlying mechanisms requires identification and characterization of all of the motor proteins involved. The recently completed DNA sequence of the *S. cerevisiae* genome revealed the complete set of kinesin-related proteins in this eukaryote. The sixth and final *S. cerevisiae* protein with substantial homology to the force-generating domain of kinesin is encoded by a previously undescribed open reading frame. Here we report that this protein, named Kip3p, is required for the first phase of nuclear migration: alignment of the mitotic spindle along the mother–daughter axis and movement of the preanaphase nucleus to the bud neck. We show that loss of dynein function has little effect on preanaphase nuclear migration and spindle orientation and that loss of *KIP3* function has little effect on movement of the anaphase nucleus through the bud neck. Kip3p is located on both astral and nuclear microtubules at all stages of the cell cycle. Kip3p is essential in strains lacking kinesin-related Kar3p and in strains lacking dynein heavy chain, indicating that Kip3p performs overlapping or dependent functions with Kar3p and dynein.

Materials and Methods

Strains, Media, and Genetic Techniques

Genotypes and sources of the strains and plasmids used in this study are listed in Table I. Strains were constructed by standard genetic methods (Rose et al., 1990) and as described in the text. The yeast media used were SD minimal medium and sporulation medium supplemented with adenine, uracil, and appropriate amino acids; SC complete medium containing 5-fluoroorotic acid (5-FOA)[1] (1 mg/ml); and YPD rich medium (Rose et al., 1990). The frequency of chromosome loss was assayed by scoring *kip3/kip3* and wild-type diploid strains for loss of heterozygosity at the mating type locus of chromosome III. The diploid strains were mated to *MAT***a** and *MAT*α tester strains on YPD plates and replica printed to score prototrophic triploid colonies (Spencer et al., 1990). Sensitivity to benomyl was tested on YPD medium containing 1% DMSO and the desired concentration of benomyl (E.I. du Pont de Nemours, Wilmington, DE). Strains expressing the Nuf2p–green fluorescent protein (GFP) fusion protein for localization of spindle poles (Kahana et al., 1995) were constructed by integrating the *NUF2–GFP* gene fusion at the *NUF2* locus using plasmid pJK67 (a gift of J. Kahana and P. Silver, Dana Farber Cancer Institute, Boston, MA). The *NUF2–GFP* gene fusion is expressed from the *NUF2* promoter, and the GFP gene contains S65T and V163A mutations.

KIP3 Deletion Construction, Gene Recovery, and Epitope Tagging

A precise deletion of the *KIP3* open reading frame (*kip3Δ*) was constructed by PCR (Baudin et al., 1993). The 3′ ends of primers 1 and 2 contained sequences for PCR amplification of the *HIS3* or *TRP1* genes present in pRS403 or pRS404 (Sikorski and Hieter, 1989), and the 5′ ends of the primers contained sequences immediately flanking the *KIP3* gene. Primer 1 was of sequence 5′-ACTTGAGTTTTCTTTCCAGCTGTATACTATTGACACTAAC**GAATTC**GATTGTACTGAGAGTGCACC-3′, and primer 2 was of sequence 5′-GAAAGAAGTTATATTCGATAGTTTACGTAGGATATGTATG**GAATTC**CTGTGCGGTATTTCACACC-3′. (Sequences flanking *KIP3* are underlined, and EcoRI restriction sites are in bold type.) The *KIP3* locus in a diploid yeast strain was replaced by this PCR product using the one-step gene replacement procedure (Rothstein, 1983). Correct recombinants were identified by PCR amplification and restriction digest analysis of genomic DNA. The primers used were primer 3, 5′-CCG**GGATCC**GACTCTTCTAATTGGTCTCT-3′ and primer 4, 5′-GGC**GTCGAC**GTCTCCTGAGAAACGTTTT-3′. (BamHI and SalI restriction sites are in bold type.)

To recover the *KIP3* gene, we screened a library of *S. cerevisiae* genomic DNA fragments cloned into the vector YCp50 (*URA3 CEN ARS*) by colony hybridization using a radiolabeled probe. The probe was a 556-bp sequence adjacent to the 5′ end of *KIP3* that was prepared from a plasmid carrying the *kip3Δ1::HIS3* allele using the EcoRI and BamHI sites introduced by primers 1 and 3. We identified a single plasmid that carried the full-length *KIP3* gene on a 10–15-kb genomic DNA insert (pDR605) out of ~4,100 colonies screened.

For epitope tagging of *KIP3*, the myc tag coding sequence (Evan et al., 1985) was introduced into the *KIP3* coding sequence as follows. A 3.8-kb fragment containing the entire *KIP3* open reading frame, but lacking the termination codon, was generated by PCR using the Expand High Fidelity PCR system (Boehringer Mannheim Corp., Indianapolis, IN). This fragment was cloned into a vector containing six tandem copies of the myc tag (pB896 [Li, 1997]). The resulting construct contained 1,419 bases of 5′ noncoding sequence, the entire *KIP3* open reading frame, and the sequence encoding the myc epitopes just 5′ of the termination codon. To eliminate the possibility of PCR-generated errors, a 2.25-kb fragment of

1. *Abbreviations used in this paper*: 5-FOA, 5-fluoroorotic acid; DAPI, 4,6-diamidino-2-phenylindole; DIC, differential interference contrast; GFP, green fluorescent protein; ts, temperature-sensitive.

Table I. Strains and Plasmids Used

Strain or plasmid*	Genotype‡
DS49	***a*** *trp1Δ1 kip1Δ1::HIS3 cin8-101*
DS118	*α trp1Δ1 kip1Δ1::HIS3* pMR1895 *(KIP1 URA3 CEN ARS)*
DS138	***a*** *trp1Δ1*
DS140	*α trp1Δ1*
DS141	*α trp1Δ1 ade2-101*
DS276	*α trp1Δ1 ade2-101 kar3Δ102::LEU2* pMR820 *(KAR3 URA3 CEN ARS)*
DS379	***a*** *trp1Δ1 cin8-112::TRP1* pDR33 *(CIN8 URA3 CEN ARS)*
DS613	***a*** *ade2-101 kip3Δ1::HIS3*
DS614	*α trp1Δ1 ade2-101 kip3Δ1::HIS3*
DS667	***a*** *trp1Δ1 kip3Δ2::TRP1* pDR605
DS689	***a*** *trp1Δ1 kip1Δ1::HIS3 cin8-101 kar3Δ102::LEU2*
DS716	***a*** *trp1Δ1 kip3Δ1::HIS3 kar3Δ102::LEU2* pDR605
DS723	***a*** *trp1Δ1 NUF2-GFP:URA3*
DS730	***a*** *trp1Δ1 ade2-101 dyn1Δ::HIS3*
DS732	***a*** *trp1Δ1 kip3Δ2::TRP1 dyn1Δ::HIS3* pDR605
DS737	*α kip1Δ1::HIS3 cin8-101 kip3Δ1::HIS3*
DS738	***a*** *trp1Δ1 ade2-101 dyn1Δ::HIS3 kip3Δ1::HIS3* pDR605
DS743	*α trp1Δ1 ade2-101 dyn1Δ::HIS3 kar3Δ102::LEU2* pMR820 *(KAR3 URA3 CEN ARS)*
DS749	***a*** *trp1Δ1 ade2-101 dyn1Δ::HIS3 kip3Δ1::HIS3* pB893
DS750	***a*** *trp1Δ1 kar3Δ102::LEU2 kip3Δ1::HIS3* pB893
DS752	***a*** *trp1Δ1 kip3Δ1::HIS3 kar3Δ102::LEU2* pDR634 *(kip3-30 TRP1 CEN ARS)*
DS765	***a*** *trp1Δ1 kip3Δ1::HIS3 dyn1Δ::HIS3* pDR636 *(kip3-20 TRP1 CEN ARS)*
DS786	*α trp1Δ1 kip3Δ1::HIS3 NUF2-GFP:URA3*
DS940	*α trp1Δ1 ade2-101 dyn1Δ::HIS3 NUF2-GFP:URA3*
MS2309	*α ura3-52 leu2-3,112 his3Δ200 ade2-101 kip2D1::URA3*
SLY57	*α ura3-52 leu2-3,112 his4 trpl smy1Δ2::LEU2*
pDR605	*KIP3* on a 10–15-kb genomic DNA fragment *URA3 CEN ARS*
pB893	*KIP3 TRP1 CEN ARS*
pB956	*KIP3-6MYC TRP1 CEN ARS*
pDR622	*KIP3 URA3 CEN ARS*

*Strains named with the DS prefix were constructed for this study or are from the Roof laboratory collection and are derivatives of strain S288C. MS2309 is from Roof et al. (1992) and SLY57 was obtained from S. Lillie and S. Brown (University of Michigan, Ann Arbor, MI). Yeast genes carried on plasmids are indicated in parentheses after the plasmid name. In general, *URA3 CEN ARS* plasmids were segregated on 5-FOA medium before experimentation except where indicated in the text.

‡All indicated DS strains carry the *ura3-52, leu2-3,112* and *his3Δ200* mutations.

wild-type *KIP3* was used to replace most of the PCR-generated clone. The remaining PCR-generated *KIP3* sequences were verified using DNA sequencing. *KIP3-6MYC* (pB956) appears to be functional, as it fully complements the lethality of *kip3Δ kar3Δ* and *kip3Δ dyn1Δ* strains using the plasmid shuffle test described below.

Tests of Synthetic Lethality

To test whether the *kip3Δ* mutation was lethal in combination with other mutations, we generally constructed double mutants in the presence of a plasmid-based wild-type copy of one of the genes and then determined whether the strain remained viable after plasmid loss. The presence of the wild-type gene during strain construction prevented the potential isolation of aneuploid strains because of genomic instability. Synthetic lethality of *kip3* and *dyn1* mutations was tested by replacing the wild-type *DYN1* gene with the *dyn1Δ::HIS3* deletion allele (from plasmid p2-1H, a gift of E. Yeh and K. Bloom, University of North Carolina, Chapel Hill, NC) in the *kip3Δ* strain DS667, which carries the *KIP3 URA3* plasmid pDR605, using one-step gene replacement. Correct deletion of *DYN1* was confirmed by restriction analysis and Southern blotting of genomic DNA. Five independently constructed double mutants were inviable when plated on 5-FOA medium, which selects against cells carrying the *URA3* plasmid (Boeke et al., 1987), indicating that *kip3* is synthetically lethal with *dyn1*.

Synthetic lethality of *kip3* with *kar3* was tested by crossing a *kip3Δ::HIS3* strain with strain DS276 containing *kar3Δ102::LEU2* and a *KAR3* plasmid. The resultant diploid strain was sporulated, and the tetrads were dissected. The spores were 83% viable, and all 11 viable *kip3 kar3* spores carried the *KAR3* plasmid. An additional 16 inviable spores were inferred to carry both the *kip3* and *kar3* mutations based on analysis of markers in the remaining spores of each tetrad; these spores may have been inviable because they did not inherit the *KAR3* plasmid. The viable *kip3 kar3* strains were sensitive to 5-FOA at 30°C, indicating that the *KAR3* plasmid was essential and that *kip3* is synthetically lethal with *kar3.* In a second test of synthetic lethality, a diploid strain homozygous for *kip3* and heterozygous for *kar3* was sporulated, and tetrads were dissected. Two spores in each tetrad were *kip3 KAR3* and viable, and two spores inferred to be *kip3 kar3* germinated and divided two to six times before ceasing growth, confirming lethality of the double mutant.

Synthetic lethality of *kip3* with *kip1* and *cin8* was tested by crossing a *kip3Δ::HIS3* strain with strain DS118 containing *kip1Δ1* and a *KIP1* plasmid, and strain DS379 containing *cin8Δ112* and a *CIN8* plasmid. The resultant diploid strains were sporulated, and 24 tetrads from each strain were dissected. The spores were >90% viable, and double *kip3 kip1* and *kip3 cin8* mutants were recovered at a frequency of ~25%. Some of the double mutants did not contain the complementing plasmid, and those that did were resistant to 5-FOA, indicating the plasmid was not essential. The *kip3 kip1* and *kip3 cin8* double mutants were capable of vegetative growth at 16, 23, 30, and 37°C, indicating that *kip3* is not synthetically lethal with *kip1* or *cin8.*

Synthetic lethality of *kip3* with *kip2* and *smy1* was tested by crossing *kip3Δ* strains with *kip2Δ* strain MS2309 or *smy1Δ* strain SLY57. The resultant diploid strains were sporulated, and 24 tetrads were dissected. The spores were >90% viable, the *kip3 kip2* and *kip3 smy1* double mutant progeny were recovered at a frequency of ~25%, and the double mutants were capable of vegetative growth at 16, 23, 30, and 37°C, indicating that *kip3* is not synthetically lethal with *kip2* or *smy1.*

Synthetic lethality of *dyn1* with *kar3* was tested by crossing a *kar3Δ* strain bearing a *KAR3* plasmid (strain DS276) with the *dyn1Δ* strain DS730. The resultant diploid was sporulated, and tetrads were dissected. Spore viability was 65%, and only 5 out of 24 tetrads yielded 4 viable spores that exhibited 2:2 segregation of mating type and the three auxotrophic markers present. Three *dyn1 kar3* double mutants were recovered from these valid tetrads, and each double mutant carried the *KAR3* plasmid. The double mutants were unable to grow on medium containing 5-FOA at 30°C, indicating that the plasmid was essential and that *dyn1* and *kar3* are synthetically lethal.

Construction of kip3 Temperature-sensitive Alleles

A 4,822-bp EcoRI/SpeI fragment from plasmid pDR605 was subcloned into the EcoRI and SpeI sites of pRS314 (*TRP1 CEN ARS*) (Sikorski and Hieter, 1989) to yield the plasmid pB893 and further subcloned into pRS416 (*URA3 CEN ARS*) to yield plasmid pDR622. These plasmids carry the entire *KIP3* open reading frame with 1,391 bp 5′ and 966 bp 3′ flanking DNA. Hydroxylamine mutagenesis of pB893 was performed by the method of Rose and Fink (1987), and temperature-sensitive (ts) alleles of *KIP3* were obtained after transformation of strain DS738 or DS716 using the plasmid shuffle technique (Boeke et al., 1987). Transformation of the *kip3-20*(ts) *dyn1Δ* strain DS765 with the *KIP3* plasmid pDR622 complemented the temperature-sensitive growth, but transformation with the vector (pRS416) did not. This confirmed that the mutation conferring temperature-sensitive growth was in *KIP3* and that the mutation is recessive.

Morphological Observations

Cells were fixed for immunofluorescence microscopy by adding formaldehyde to 3.7% directly to the culture medium and incubating for 2 h at 23°C, or overnight at 4°C. Cells were prepared for immunofluorescence microscopy as described (Rose et al., 1990). For the Kip3p localization experiment, Kip3p-6myc was visualized with mAb 9E10, which recognizes the myc epitope (Santa Cruz Biotechnology, Santa Cruz, CA), and microtubules were visualized with the rat antitubulin antibody YOL 1/34 (Accurate Chemical and Scientific Corp., Westbury, NY). Fluorochrome-conjugated secondary antibodies were from Jackson Immunoresearch Labs, Inc. (West Grove, PA). For double labeling of Kip3p and microtubules, controls demonstrated that cross-reactivity and light channel spill-over did not contribute to the final images when species-specific secondary anti-

bodies were used. For all other immunofluorescence experiments, tubulin was stained with the antitubulin monoclonal antibody BIBE2, a gift of F. Solomon (Massachusetts Institute of Technology, Cambridge, MA). The secondary antibody was FITC-conjugated goat anti–mouse antibody (Accurate Chemical and Scientific Corp.), which was absorbed against fixed yeast cells for 3 h at 4°C before use to minimize background signal. DNA was stained using 4,6-diamidino-2-phenylindole (DAPI) (Boehringer Mannheim Corp.). To observe Nuf2p–GFP localization in fixed cells, cells in culture medium were fixed for 1 h with 3.7% formaldehyde, washed, and applied to polylysine-treated Teflon®-masked slides for viewing.

For live cell microscopy of spindle pole body location, cells were applied to a microscope slide with a thin pad of 1% agarose containing SC complete medium, and a coverslip was applied and sealed with a thin bead of a mixture of equal parts Vaseline, lanolin, and paraffin at the edges. Cells were imaged at 23–25°C using a microscope (model DMRBE; Leica, Inc., Deerfield, IL) equipped with a 100×/1.4 NA objective, a monochrome CCD camera (Cohu Inc., San Diego, CA), a 100-W mercury vapor lamp, and a fluorescein filter set. Images were captured using LG3 frame grabber hardware (Scion Corp., Frederick, MD) and NIH Image software (written by W. Rasband and available at http://rsb.info.nih.gov/nih-image/) with a custom set of macro programs to control the camera exposure settings, fluorescence illumination shutter, and motorized microscope stage. At each time point, both differential interference contrast (DIC) and fluorescence images were photographed at three focal planes spaced at 1-μm intervals to increase the likelihood of detecting both spindle pole bodies. Illumination during fluorescence photography was controlled by a shutter and was 200 ms or less for each image.

Micrographs were spatially calibrated using NIH image software and a stage micrometer. Distance and angle measurements were made using Object Image software, a modified version of NIH Image available at the above internet site. Measurements to determine nuclear migration indices were made on digital images of cells by the method of Jacobs et al. (1988), and the statistical significance of the difference between the variances of nuclear migration indices was tested using the two-tailed variance ratio test at a 5% significance level.

Results

Predicted Structure of the Kinesin-related Gene KIP3

Upon completion of the *S. cerevisiae* genome sequencing projects, we searched the public databases using the BLAST program to identify additional kinesin-related genes. In addition to known genes *KIP1*, *KIP2*, *KAR3*, *CIN8*, and *SMY1*, this search detected an open reading frame on chromosome VII (YGL216w) that is predicted to encode an 805–amino acid protein of molecular mass 91 kD. Residues 86–464 showed 39% identity to the motor domain of human kinesin and include putative ATP-binding and microtubule-binding motifs (Fig. 1 *A*). Using the nomenclature employed for the kinesin-related genes *KIP1* and *KIP2*, we have designated this gene *KIP3.* Subfamilies of kinesin-related proteins have been defined by exceptionally high sequence conservation in the motor domain (Moore and Endow, 1996), but sequence comparisons with Kip3p did not reveal any obvious subfamily relationship. The nonmotor, COOH-terminal 340 amino acids did not exhibit obvious sequence similarity to the nonmotor regions of other kinesin-related proteins, nor to any other protein in the current DNA, protein, and EST databases. The COOH-terminal domain contains several regions predicted to form α-helical coiled coils that potentially mediate protein multimerization (Fig. 1 *B*).

KIP3 Is Not Essential for Mitosis, Meiosis, or Karyogamy

No known mutations map to *KIP3.* Therefore, to determine the function of *KIP3* a deletion mutant was made by replacing the *KIP3* coding sequence with the *HIS3* gene in a diploid strain via one-step gene replacement (see Materials and Methods). Tetrad analysis demonstrated that *KIP3* is not essential for mitotic growth. The efficiency of karyogamy was tested by crossing a *kip3Δ* mutant to wild-type and *kip3Δ* strains in a qualitative limited mating assay (Conde and Fink, 1976) and was found to occur at the

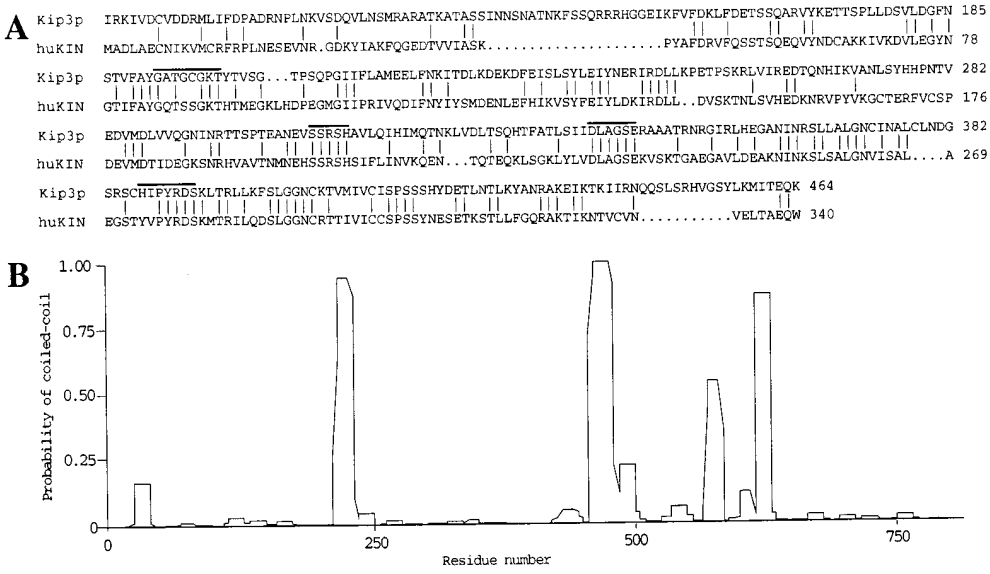

Figure 1. Kip3p sequence alignment and coiled-coil formation probability. (*A*) Alignment of Kip3p residues 86-464 with human kinesin (*huKIN*) (Navone et al., 1992) residues 1–340 was performed using the Gap program (Genetics Computer Group, Inc., Madison, WI). Vertical lines indicate amino acid identities, and dots indicate gaps introduced to improve alignment. Horizontal lines indicate key residues of the ATP-binding site (GX_4GKT) and amino acids suspected to play a role in nucleotide phosphate sensing and microtubule binding. (*B*) The probability of coiled-coil formation in the predicted Kip3p amino acid sequence was calculated using the algorithm of Lupas et al. (1991) with a window size of 14 amino acids.

Table II. Cell-Type Distributions of Wild-Type and Mutant Cultures

Relevant genotype‡	Temperature	Cells with the illustrated distribution of nuclear DNA (%)*						
		UB	SB	MD	ASE	BNM	BN	AN
	°C							
WT	11	59	24	4	11	1	0	0
	30	32	45	3	19	0	0	0
	37	51	35	3	10	0	0	0
kip3Δ	11	43	18	5	12	15	4	3
	30	36	31	8	19	4	1	1
	37	39	25	14	9	6	2	5
dyn1Δ	11	43	12	0	2	15	16	12
	30	43	22	3	10	12	2	9
	37	46	19	13	5	6	5	6
kar3Δ	11	48	16	23	2	0	5	6
	30	36	15	44	6	0	2	4
	37	36	8	45	5	0	2	4
kip3(ts) *dyn1Δ*	37	16	27	35	3	10	3	6
kip3(ts) *kar3Δ*	37	35	17	34	2	2	2	7

*Abbreviations: *UB*, unbudded cells with a single nuclear DNA mass; *SB*, small-budded cells with a single nuclear DNA mass (bud diameter <0.5 mother diameter); *MD*, metaphase-delayed cells with a large bud and a single nuclear DNA mass (bud diameter >0.5 mother diameter); *ASE*, normal anaphase spindle elongation; *BNM,* binucleate mother cells undergoing anaphase spindle elongation within the mother cell; *BN*, unbudded binucleate cells; *AN*, unbudded anucleate cells.

‡WT (DS141), *kip3Δ1* (DS613), *dyn1Δ* (DS730), and *kar3Δ102* (DS276) strains were grown to mid-logarithmic phase by diluting a culture grown at 30°C to A_{600} = 0.1 and incubating for 16 h at 11°C (final A_{600} = 0.3) or for 5 h at 30 or 37°C (final A_{600} = 0.5). *kip3-20*(ts)*dyn1Δ* (DS765) and *kip3-30*(ts)*kar3Δ102* (DS752) strains were prepared by diluting a 30°C culture to A_{600} = 0.1 and incubating at 30°C until the A_{600} = 0.5, when the culture was shifted to 37°C for 4 h. Cells were prepared for DIC and fluorescence microscopy as described in Materials and Methods, and >150 cells were counted for each strain and temperature.

wild-type efficiency. Meiosis was tested by sporulating the homozygous *kip3Δ* diploid strain and dissecting the tetrads. The efficiency of sporulation was normal and spore viability was >90%. Chromosome instability was tested using homozygous *kip3Δ* diploid strains in a qualitative assay for chromosome III loss and was found to occur at the wild-type frequency.

To investigate potential functions of *KIP3* that are not essential for viability, we examined mitotic cultures of the *kip3Δ* mutant in more detail. The growth rate of the *kip3Δ* mutant at 30 and 37°C in liquid YPD medium was the same as an isogenic wild-type strain, and flow cytometry showed that the mutant cultures at 30 and 37°C had the same proportion of G1 and G2 cells as wild-type cultures. However, a subtle cell cycle delay that was not evident from flow cytometry analysis was evident from the analysis of cell morphology shown in Table II, where there was an increased frequency of preanaphase cells whose buds had grown beyond the size at which nuclear division normally occurs. Cells defined as delayed in metaphase had a single nucleus and a bud >50% the diameter of the mother cell. In the wild-type strain, cells delayed in metaphase comprised 3–4% of the culture, while in the *kip3Δ* mutant these cells comprised 5–14% of the culture, depending on incubation temperature.

Increased Microtubule Stability in kip3 Mutants

Mutation of genes that regulate microtubule function often results in altered sensitivity to drugs that destabilize microtubules (Stearns et al., 1990). Sensitivity of the *kip3Δ* mutant to the antimicrotubule drug benomyl was tested by spotting known numbers of cells on YPD plates containing different concentrations of benomyl (Fig. 2). Both the wild-type and mutant strains exhibited substantial growth at 30°C on 0–20 μg/ml benomyl, while only the *kip3Δ* mutant grew at 30 μg/ml benomyl, indicating that *kip3* mutants are more resistant to benomyl than wild-type. A similar degree of increased resistance to benomyl occurred in an isogenic strain containing a deletion mutation of the kinesin-related gene *KAR3.* The same relative pattern of increased resistance of the *kip3Δ* mutant was observed when the plates were incubated at 23 or 37°C. Consistent with increased microtubule stability in the *kip3Δ* mutant, immunofluorescent localization of tubulin in the *kip3Δ* mutant showed brighter staining of astral microtubules in the *kip3Δ* mutant than in wild-type (Fig. 3). In budded *kip3Δ* and wild-type cells, the astral microtubules extended from the nucleus and passed through the neck into the bud.

kip3 Mutants Are Defective in Migration of the Nucleus to the Bud Neck

In addition to nuclear division, meiosis, and karyogamy, microtubule function is required for migration of undivided nuclei to a site near the neck of the newly emerging daughter bud, and for the subsequent insertion of nuclei into the neck as spindle elongation begins (Huffaker et al., 1988; Jacobs et al., 1988; Snyder et al., 1991; Yeh et al.,

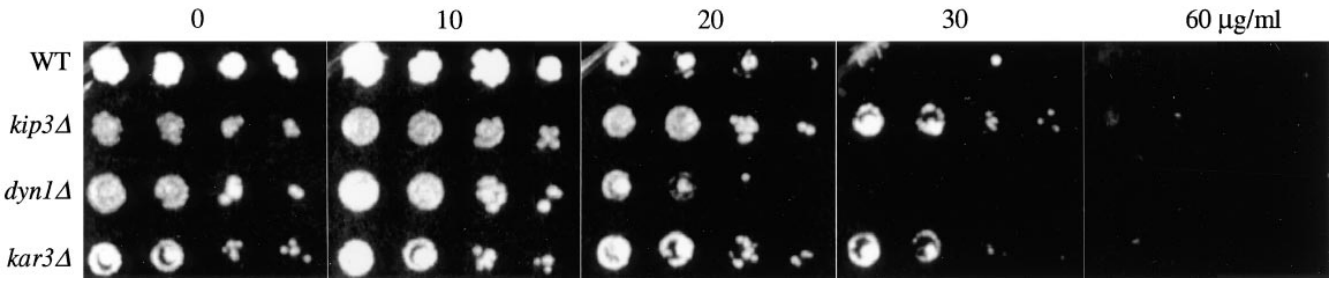

Figure 2. Increased benomyl resistance in the *kip3Δ* mutant. Strains wild-type (DS140), *kar3Δ102* (DS276), *kip3Δ* (DS614), and *dyn1Δ* (DS730) were incubated at 23°C for 2 d in liquid YPD medium. Serial dilutions were prepared, and ~10^4, ~10^3, ~10^2, and ~10 cells were spotted in horizontal rows on solid YPD medium containing 1% DMSO and benomyl at the indicated concentration and photographed after 3 d of growth at 30°C.

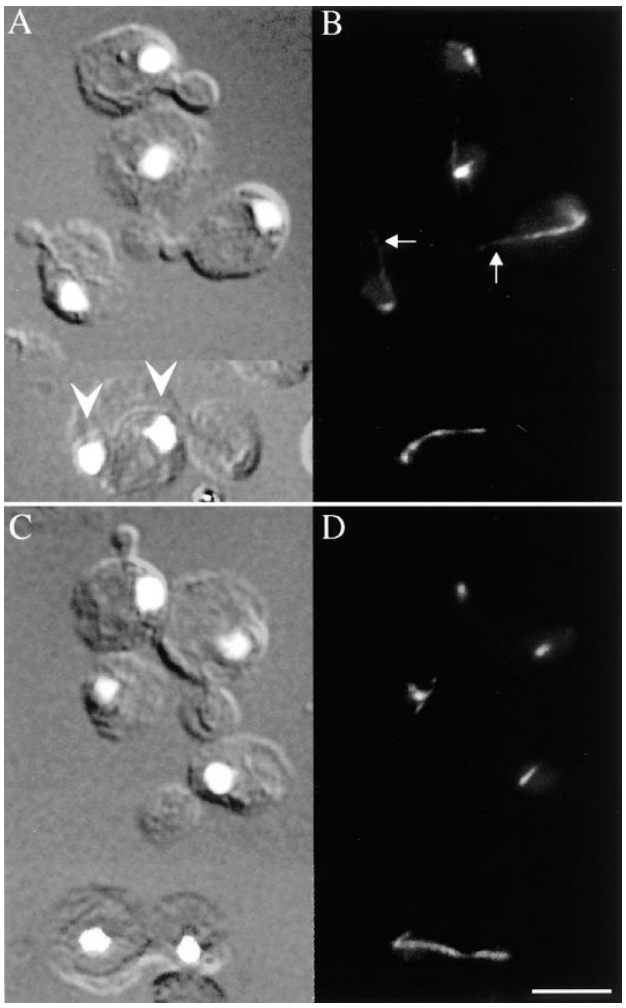

Figure 3. Disruption of *KIP3* affects nuclear migration. *kip3Δ* strain DS614 (*A* and *B*) and wild-type strain DS141 (*C* and *D*) were grown in YPD medium at 30°C to mid-logarithmic phase and prepared for immunofluorescence microscopy. (*A* and *C*) DIC images overlaid with corresponding DAPI-stained images to show position of nuclear DNA. (*B* and *D*) Antitubulin staining to visualize microtubules. *A* and *B* show *kip3Δ* cells with nuclei located distal to the neck and with brightly staining astral microtubules extending into the bud (*arrows* in *B*). Also present is a mother cell with two nuclei (*arrows* in *A*) that are still connected by a mitotic spindle. The small-budded wild-type cells in *C* and *D* contain significantly fewer prominent astral microtubules. Bar, 5 μm.

1995). Anaphase spindle insertion into the bud neck requires dynein function, but no microtubule-based motor protein has yet been shown to be required for migration of the nucleus to the neck of the emerging bud. We examined nuclear migration in the *kip3Δ* mutant using DIC and fluorescence microscopy of fixed cells and found that the *kip3Δ* mutant was defective in positioning nuclei within the cell, both before and during anaphase.

To assess nuclear migration before anaphase, we measured the nucleus-to-neck distance in budded cells with undivided nuclei. The nucleus-to-neck distances were measured on digital micrographs and were corrected for differences in the sizes of the mother cells using the nuclear migration index, which is a ratio of these two values (Jacobs et al., 1988). Fig. 3 shows representative cells, and Fig. 4 shows histograms of the number of cells observed with a given nuclear migration index. Wild-type cells from exponentially growing populations exhibited the expected nonrandom placement of nuclei near the bud neck; when the culture was grown at 30°C, the mean distance between the proximal edge of the nuclear DNA mass and the bud neck was 1.1 ± 0.66 μm (mean ± SD) and the corresponding nuclear migration index was 0.17 ± 0.093 (Fig. 4). In contrast to wild-type, the *kip3Δ* mean distance between the nucleus and bud was 1.8 ± 1.3 μm, and the corresponding nuclear migration index was 0.23 ± 0.17. The larger standard deviation observed with the *kip3Δ* mutant is due to the fact that undivided nuclei tended to be positioned more randomly in the mother cell, with larger populations of cells with the nucleus located both more closely and more distantly to the neck (Fig. 4). A variance ratio test demonstrated that the differences were significant for cultures grown at 11, 30, and 37°C.

To examine potential defects of the *kip3Δ* mutant in positioning the nuclei during anaphase spindle elongation, we used DIC and fluorescence microscopy to score the frequency of mother cells that contained two nuclei. In wild-type cells that contain two nuclei, one nucleus is found within the mother and another is found in the daughter. In contrast, 15% of the *kip3Δ* cells grown at 11°C contained both nuclei within the mother cell (Table II). The binucleate cells comprised 55% of the anaphase stage cells in the asynchronously growing culture. Microtubules were observed using tubulin immunofluorescence microscopy, and we found that all binucleate mother cells with an empty bud contained an intact mitotic spindle connecting the two nuclear DNA masses (Fig. 3). Frequently, the spindle was not aligned along the mother–bud axis as in wild-type cells undergoing anaphase.

kip3 Mutants Are Defective in Preanaphase Mitotic Spindle Orientation

Because the *kip3Δ* mutant was defective in nuclear positioning, we tested whether loss of *KIP3* function also caused a defect in the potentially related process of spindle orientation. A specific orientation of the nucleus and its associated spindle pole body can be detected in wild-type cells when the bud begins to emerge and the spindle pole body faces the neck. Upon assembly of a bipolar mitotic spindle, one spindle pole is typically oriented toward the neck so that the spindle is approximately aligned along the mother–daughter axis. To investigate spindle orientation, we fixed cells from exponentially growing populations and measured the orientation of preanaphase spindles with respect to the mother–daughter axis. Spindle orientation was observed by fluorescence microscopy, using strains expressing a fusion of the spindle pole body protein Nuf2p to green fluorescent protein developed by Kahana et al. (1995). The Nuf2p–GFP fusion protein complements a *nuf2* null mutation, and strains containing the fusion grow normally and exhibit anaphase spindle elongation kinetics similar to spindle movements observed independently by DIC microscopy of live cells (Kahana et al., 1995; Yeh et al., 1995). The measurements in Fig. 5 show that the majority of preanaphase spindles in the

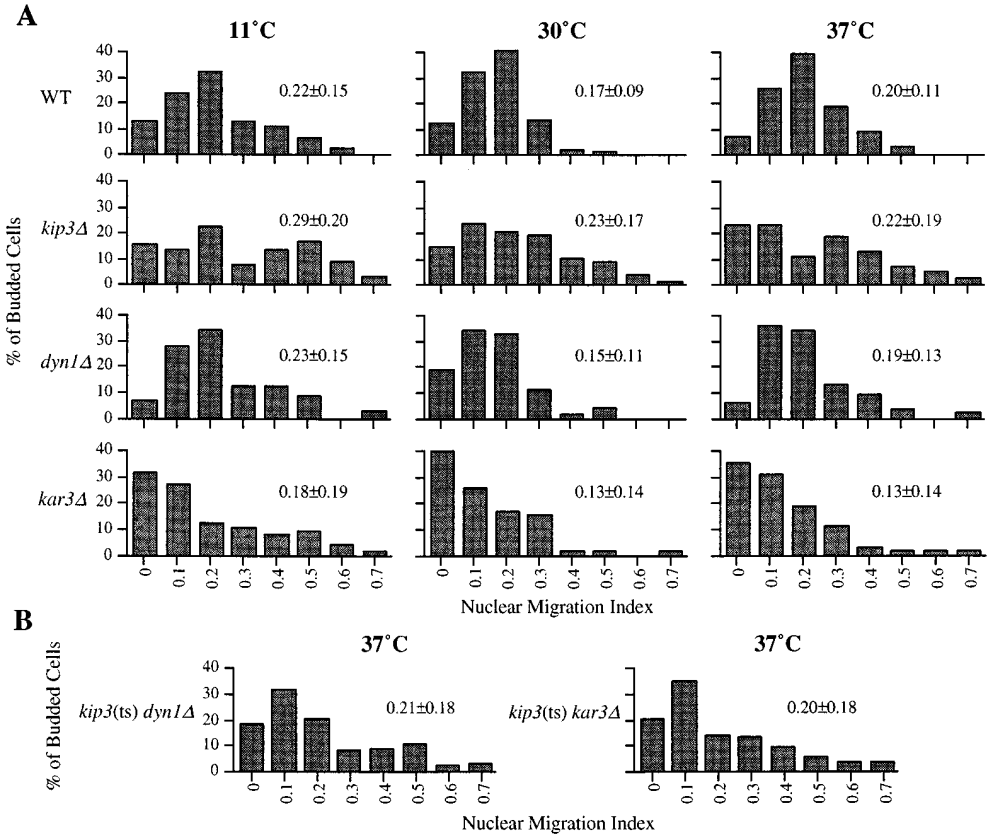

Figure 4. Loss of *KIP3* function causes mislocalization of undivided nuclei. (*A*) Histograms of nuclear migration indices of wild-type (DS141), *kip3Δ* (DS614), *dyn1Δ* (DS730), and *kar3Δ* (DS276) strains grown to mid-logarithmic phase at the indicated temperature. (*B*) Histograms of *kip3*(ts) *kar3Δ* (DS752) and *kip3*(ts) *dynΔ* (DS765) strains grown to mid-logarithmic phase at the permissive temperature of 30°C and shifted to the nonpermissive temperature of 37°C for 4 h. The mean nuclear migration index and one standard deviation (mean ± SD) is inset on each histogram. The nuclear migration index of a cell is proportional to the proximity of its nucleus to the bud neck and is calculated as the distance between the neck and the nearest edge of the nucleus visualized by DAPI staining divided by the distance between the neck and the most distal edge of the cell wall (Jacobs et al., 1988). The statistical significance of the difference between the variances of the nuclear migration indices was tested with a variance ratio test. The variance ratio for the *kip3Δ* and wild-type 30°C cultures was found to be 3.4, well above the 95% significance point of 1.5, indicating that we have significant evidence that the position of nuclei in the *kip3Δ* mutant is more random than in wild-type. The position of nuclei in the *kip3Δ* mutant grown at 11 and 37°C was also significantly more random than in wild-type. The variance ratio for the *kip3*(ts) *dyn1Δ* double mutant and wild-type cultures was 2.5, above the 95% significance point of 1.5, but there was no significant difference between the *kip3*(ts) *dyn1Δ* double mutant and the *kip3Δ* single mutant. 50–100 cells were measured for each strain and temperature.

wild-type strain were oriented within 30 degrees of the mother–daughter axis, while the preanaphase spindles in the *kip3Δ* mutant were nearly randomly oriented. Thus, *KIP3* function is required for normal preanaphase spindle orientation.

Before Anaphase, kip3 Mutants Exhibit Large Oscillations in Nuclear Position

The pathway of nuclear migration begins at the end of anaphase when the spindle pole bodies of the newly divided nuclei are positioned distal to the neck. After mitotic spindle disassembly, the nuclei migrate to a position ~1 μm from the neck of the new bud. In haploid cells, the site of bud emergence is usually adjacent to the previous division site (axial budding pattern), necessitating that the nucleus traverse the diameter of the cell. The timing of this event in the cell cycle and the path and rate of movement is not apparent by examining populations of fixed cells because there is not yet a bud to provide a temporal and spatial reference point. However, by observing movement of the nucleus in a live cell after anaphase, the timing, path, and rate of nuclear movement can be investigated. To observe mitotic spindle pole movements in live cells, we used time-lapse fluorescence microscopy of strains expressing the Nuf2p–GFP fusion (Kahana et al., 1995). We collected both fluorescence and DIC images at three focal planes at each time point and overlaid the fluorescence images of spindle poles on the corresponding DIC images of cells to accurately position the spindle poles within the cell.

To examine nuclear migration in haploid G1 phase cells, we monitored the position of the spindle pole body relative to the prebud site after anaphase. In wild-type cells after maximal anaphase spindle pole separation, the spindle pole body typically moved 1–2 μm toward the cell center in 4 to 8 min (Fig. 6 *A*). This immediate and rapid movement preceded cytokinesis and probably corresponds to a similar movement described previously in diploid cells (Yeh et al., 1995). After the rapid movement, the spindle pole body in wild-type cells typically traversed an additional 2–3 μm to the site near the neck within 10 to 30 min, and then its position became relatively stable until anaphase, exhibiting movements of 0.5 μm or less.

In the *kip3Δ* mutant, the initial rapid phase of spindle pole body movement after maximal anaphase spindle elongation appeared similar to that of wild-type strains (Fig. 6). However, subsequent to the initial movement, the spindle poles exhibited large oscillations in position, with

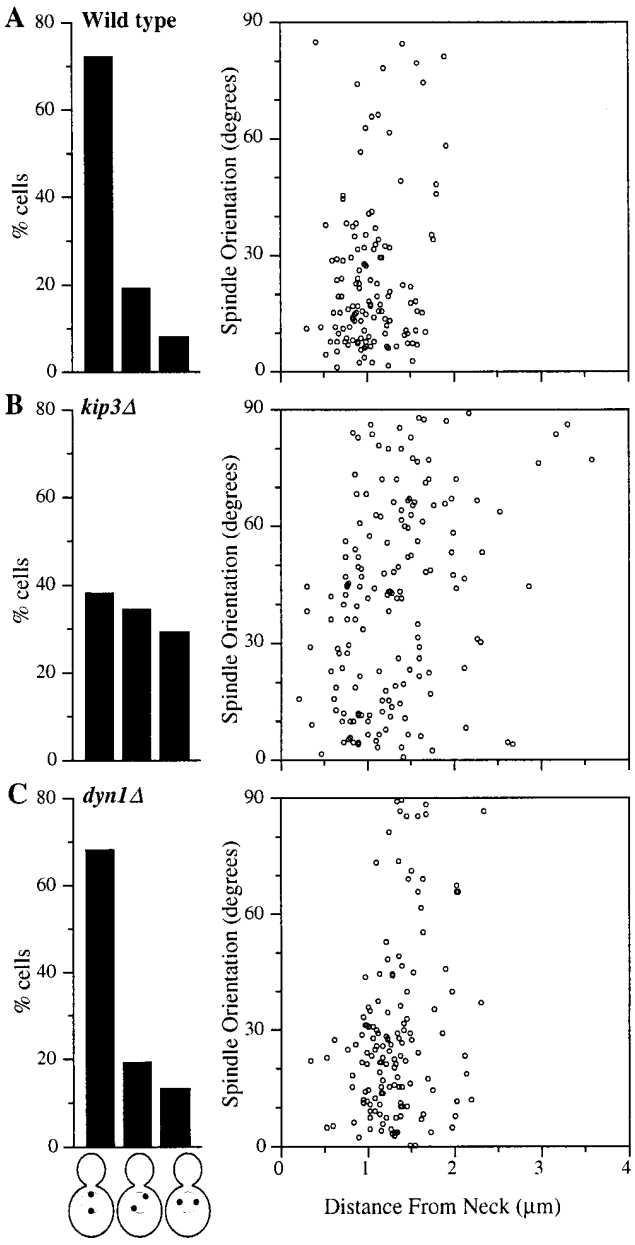

Figure 5. Loss of *KIP3* function causes misorientation of preanaphase spindles. The histograms on the left indicate the frequency of cells with bipolar spindles that are oriented from 0–30 degrees of the mother–daughter axis (*first bar*), from >30–60 degrees (*second bar*), and from >60–90 degrees (*third bar*). The scatter plots on the right contain all of the data shown in histogram format and in addition show the relationship between spindle orientation and distance between the neck and the neck-proximal spindle pole. There was little correlation between spindle orientation and nuclear location in all three strains. (*A*) Wild-type (DS723), (*B*) *kip3Δ* (DS786), and (*C*) *dyn1Δ* (DS940) strains were grown at 30°C in YPD medium and fixed for microscopy. The location of the spindle poles and spindle orientation was determined by overlaying images of Nuf2p–GFP fusion fluorescence onto DIC images of the corresponding cells. Spindle orientation was measured in all cells in the population that had a preanaphase spindle with both spindle pole bodies in a single focal plane and a pole-to-pole length of 0.8–1.2 μm. More than 120 preanaphase spindles from two independent cultures were measured for each strain.

the spindle pole alternately moving closer and farther from the neck. A single spindle pole body movement toward or away from the neck was typically 1.5–2.5 μm and occurred in 10–15 min (Fig. 6, *C* and *D*). The spindle pole also exhibited lateral movements that sometimes occurred without apparent large changes in the pole to neck distance (Fig. 6 *C*). The highly variable position of the spindle pole relative to the neck revealed by real-time analysis is consistent with the defective nuclear positioning shown by analysis of nuclear position in fixed cells. Furthermore, the variable nuclear positioning occasionally results in the presence of the nucleus near the neck, constituting an alternate pathway for nuclear migration that could account for the viability of *kip3* mutants.

Nuclear Segregation during Anaphase Proceeds Normally in the kip3 Mutant

Microscopy of individual live cells has revealed several discrete phases of spindle elongation (Palmer et al., 1989; Kahana et al., 1995; Yeh et al., 1995; Yang et al., 1997). When the initial fast phase of anaphase commences, spindle elongation moves one pole of the mitotic spindle to the neck, and the nucleus passes through the narrow opening. The fast phase of elongation continues until the spindle is ~4 μm long, and then elongation continues at a slower rate, sometimes with a pause between the two phases. To determine whether loss of *KIP3* function affects the kinetics of spindle elongation, we used live cell microscopy of the Nuf2p–GFP fusion to observe these movements in a *kip3Δ* mutant. To focus specifically on anaphase, cells with a short bipolar spindle located near the neck were selected for time-lapse photography. The average rates of fast and slow spindle elongation were similar in wild-type and *kip3* strains (Fig. 7 *A*). Fast elongation in the *kip3* mutant was 0.69 ± 0.25 μm/min (n = 10) over the first 6–8 min of elongation, and in the wild-type strain it was 0.60 ± 0.19 μm/min (n = 6). Slow elongation in the *kip3* mutant was 0.14 ± 0.06 μm/min (n = 6), and in the wild type strain it was 0.14 ± 0.08 μm/min (n = 4). Thus loss of *KIP3* function does not dramatically affect anaphase B kinetics.

During the early period of anaphase spindle elongation, when the dividing nucleus is in the neck, the nucleus and spindle can exhibit forward and reverse motion along the mother–daughter axis. These movements range in distance from 0.5–1 μm in wild-type diploid cells, and they are absent in *dyn1* mutants (Yeh et al., 1995). We observed few forward and reverse motions of the nucleus relative to the neck in the *dyn1* mutant, but we did observe such movements in wild-type and *kip3* strains (Fig 7, *B–I*), suggesting that *KIP3* is not essential for these movements.

The early anaphase spindle undergoes proportionally greater elongation before insertion of the nucleus into the neck in *dyn1* mutants compared to wild-type (Yeh et al., 1995). To identify possible defects in this process in the *kip3* mutant, we measured the pole-to-pole length of the spindle at the time that the daughter-bound pole passed through the neck (Fig. 7). Some elongation of the spindle occurred before insertion into the neck in all strains examined. Spindle length upon neck contact in the *kip3* mutant was 2.9 ± 0.8 μm (n = 10), and in the wild-type control it was 2.3 ± 0.5 μm (n = 5). This difference in spindle

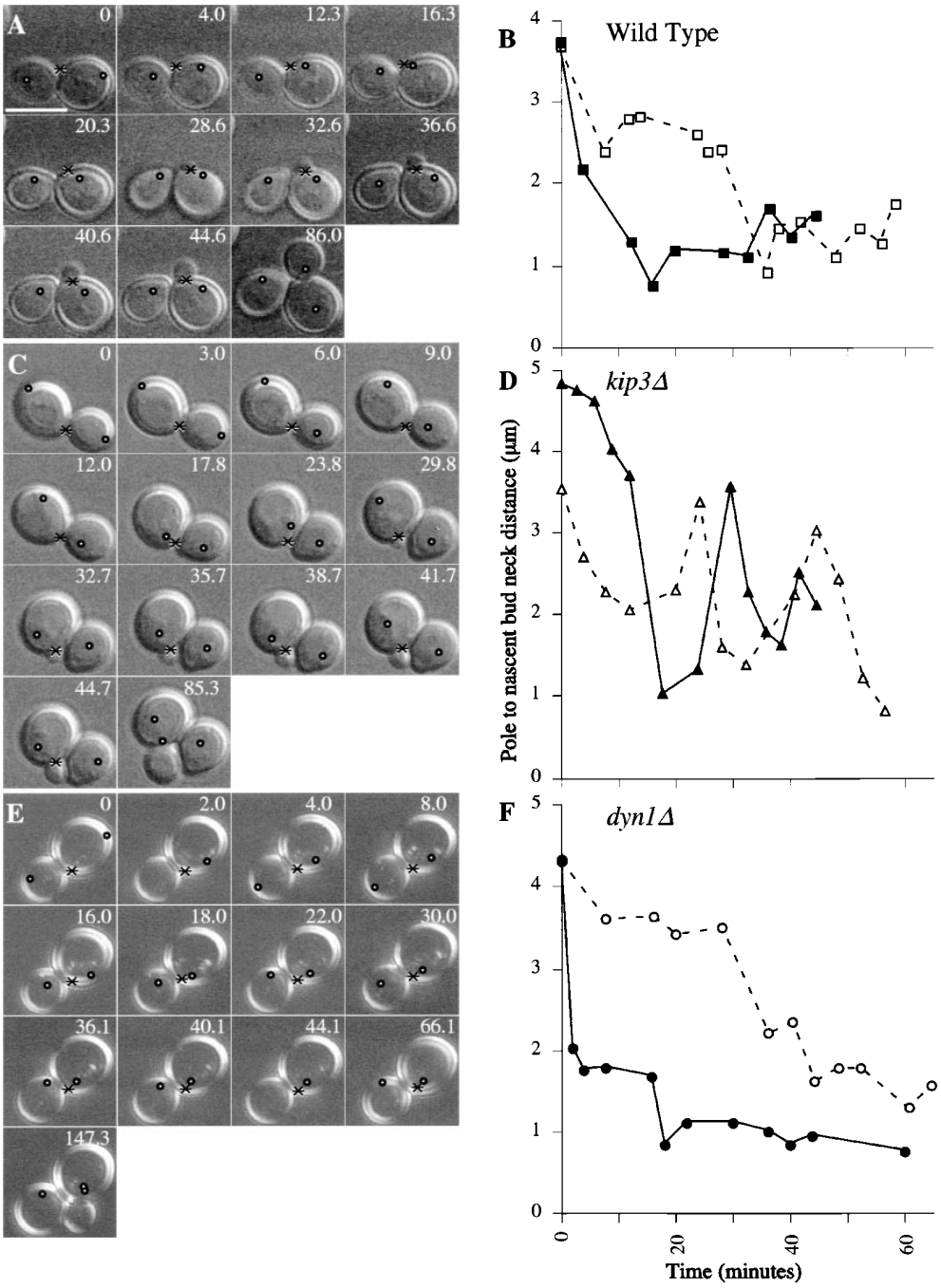

Figure 6. Large oscillations in position of nuclei after spindle disassembly in the *kip3Δ* mutant. (*A*, *C*, and *E*) A time-lapse series of DIC micrographs of wild-type (*A*), *kip3Δ* (*C*), and *dynΔ* (*E*) cells. The elapsed time (min) is indicated, and $T = 0$ is the time of maximal anaphase spindle elongation. The position of the spindle poles is indicated by open circle symbols, and the position of the bud neck of the new daughter cell is indicated by the asterisk. At early times in the series when the bud had not yet emerged, the prebud site was defined by comparison to later time points. Spindle pole position was defined by overlaying images of Nuf2p–GFP fluorescence onto corresponding DIC images. To obtain DIC images in which the bud was always in focus, images of two focal planes spaced 1 μm apart were projected onto a single plane. (*B*, *D*, and *F*) Two examples of the distance of the spindle pole in the mother cell from the new bud neck, plotted as a function of time. The closed symbols represent pole position in the mother cells shown in *A*, *C*, and *E*. The open symbols represent pole position from an independent set of micrographs (not shown), to convey the range of movements observed. Note that in addition to nuclear migration, small changes in pole position could also be caused by nuclear rotation. Bar, 5 μm.

lengths was not statistically significant (unpaired *t* test, $P = 0.12$), indicating that loss of *KIP3* function has little effect on insertion of the spindle through the neck. In contrast, the spindle length of an isogenic *dyn1* mutant at the time of insertion was 4.1 ± 0.7 μm ($n = 8$), which was significantly different from wild-type ($P = 0.0005$). Translocation was complete within 5 min in the wild-type, *kip3*, and *dyn1* cells observed, indicating that transient elongated nuclei at the beginning of successful anaphase events make only a small contribution to the populations of binucleate cells reported in Table II.

Loss of Dynein Function Has Little Effect on Nuclear Migration to the Neck or on Preanaphase Spindle Orientation

Mutants defective in the gene for the dynein heavy chain (*dyn1* or *dhc1*) have been reported to be defective in nuclear orientation, insertion of the dividing nucleus into the neck, and oscillatory movement of the anaphase-stage nucleus within the neck (Eshel et al., 1993; Li et al., 1993; Yeh et al., 1995). To compare the effect of loss of *KIP3* function to loss of *DYN1* function in isogenic strains, we

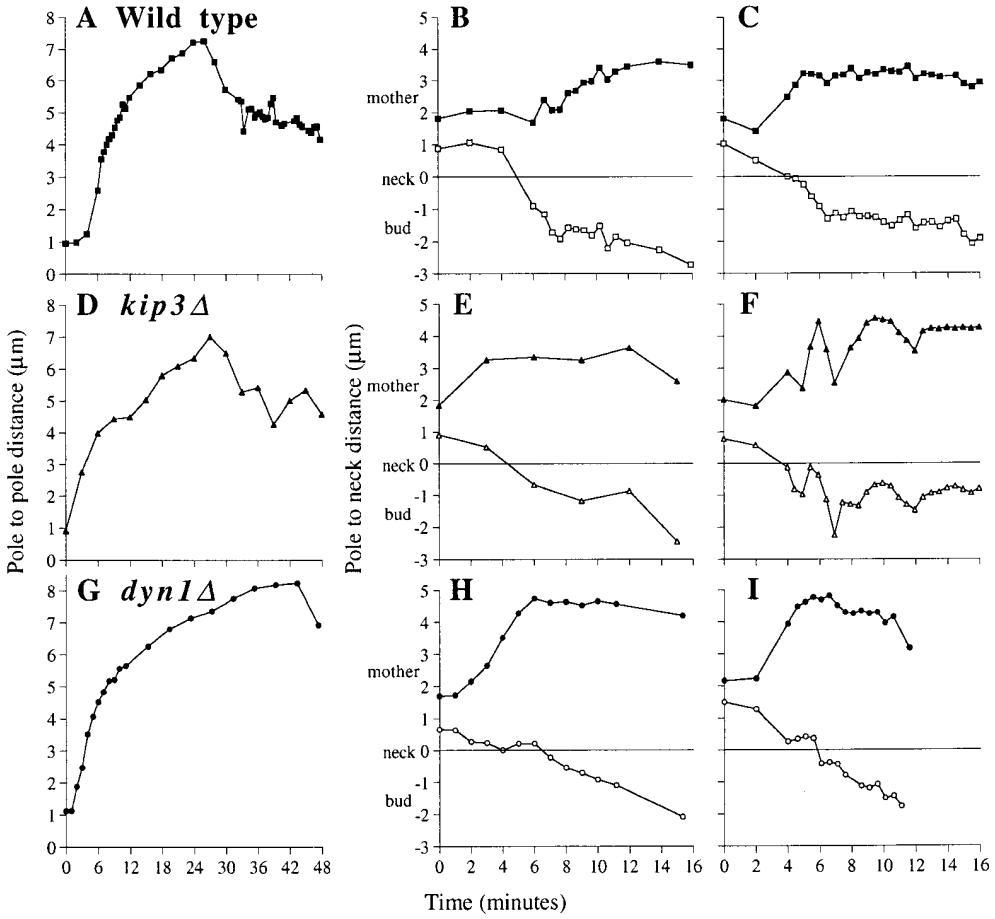

Figure 7. Normal kinetics of anaphase spindle elongation in the *kip3Δ* mutant. (*A*, *D*, and *G*) Pole-to-pole distance as a function of time in an individual cell of the indicated strain. Each cell exhibited the fast and slow phases of anaphase spindle elongation, followed by a reduction of the pole to pole distance upon spindle disassembly. (*B*, *E*, and *H*) Data from the same cells and recordings in *A*, *D*, and *G*, with the first 16 min of anaphase shown on an expanded time axis. To illustrate movement of the spindle poles relative to the neck, distances between the neck and the pole in the mother cell were plotted as positive numbers, and distances between the neck and the pole in the bud were plotted as negative numbers. (*C*, *F*, and *I*) Data recorded from different cells. Measurement of spindle pole position relative to the neck was performed on images of Nuf2p–GFP fluorescence overlaid onto corresponding DIC images. The haploid strains used were wild-type strain DS723 (*A–C*), *kip3Δ* strain DS786 (*D–F*), and *dyn1Δ* strain DS940 (*G–I*).

constructed a *dyn1Δ* mutant and scored the frequency of binucleate cells and the position of undivided nuclei within mother cells. Consistent with the previously reported defects in anaphase-stage cells, the *dyn1Δ* mutant cultures contained binucleate mother cells at a frequency of 11–31%, depending on incubation temperature (Table II). Proficiency in migration of undivided nuclei was assessed by determining the mean nuclear migration index and standard deviation. The histograms in Fig. 4 show that the *dyn1Δ* mutant grown at 11, 30, and 37°C showed a distribution of nuclear migration indices that was similar to the wild-type strain. The ratio of variances between wild-type and *dyn1Δ* strains at each temperature was below the 95% significance point, indicating no significant difference was present. Furthermore, spindle pole movement observed by microscopy of live *dyn1* cells containing the Nuf2p–GFP fusion showed that the path and rate of movement was similar in *dyn1* and wild-type cells (Fig. 6, *E* and *F*), although we did observe that the time between anaphase spindle disassembly and bud emergence was prolonged in the *dyn1* mutant. Thus, in contrast to the *kip3Δ* mutant, the *dyn1Δ* mutant is not significantly impaired in migration of undivided nuclei to the site near the bud neck. This is consistent with previous measurements of nuclear distribution in hydroxyurea-arrested *dyn1* cells, where nuclear translocation into the bud decreased, but accumulation of nuclei at the bud neck was largely unimpaired (Yeh et al., 1995).

To determine whether orientation of the preanaphase mitotic spindle is affected by loss of dynein function, we used the Nuf2p–GFP fusion protein employed above for the *kip3* mutant to measure spindle orientation in fixed *dyn1Δ* mutant cells. Preanaphase spindles in the *dyn1Δ* mutant were oriented within 30 degrees of the mother–daughter axis in 68% of the cells, compared to 72% in wild-type cells. There was a small increase in the number of cells with a spindle misoriented by 60–90 degrees (13%, compared to 8% in wild-type). Thus, loss of dynein heavy chain function has little effect on preanaphase spindle orientation.

Synthetic Lethal Interactions of the kip3Δ Mutation with Mutations in Other Microtubule-based Motor Genes

The phenotypes presented above of mutants singly defective in *KIP3* or *DYN1* indicate that *KIP3* is required for nuclear migration to the bud neck and preanaphase spindle orientation, but that *DYN1* is not. However, Kip3p and Dyn1p may perform overlapping or dependent functions that are not evident in the single mutants. For instance, the binucleate mother cell phenotype manifested

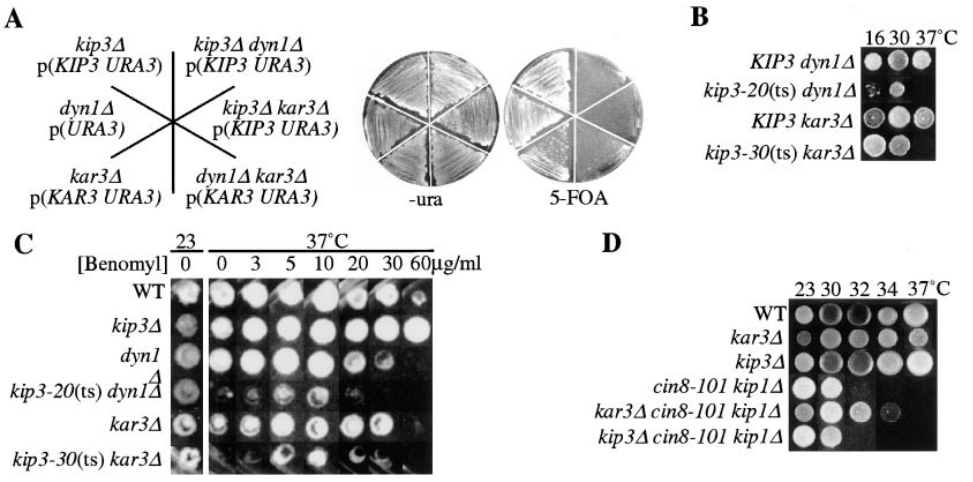

Figure 8. (*A*) Synthetic lethality of *kip3*, *dyn1*, and *kar3*. Strains *kip3*, *dyn1*, *kar3*, *kip3 dyn1* (DS732), *kip3 kar3* (DS716), and *dyn1 kar3* (DS743) carry a centromere-based plasmid with the markers indicated in parentheses. To test whether the plasmids are essential for viability, the strains were grown on YPD medium for 3 d at 30°C to allow for possible plasmid loss, the strains were plated on minimal medium lacking uracil (selects for plasmid) and on 5-FOA medium (selects against plasmid), and the plates were photographed after 3 d of incubation at 30°C. (*B*) Temperature-sensitive alleles of *kip3*. Strains *dyn1* (DS749), *kip3-20*(ts) *dyn1* (DS765), *kar3* (DS750), and *kip3-30*(ts) *kar3* (DS752) were grown to saturation and spotted on YPD medium at the indicated temperature. Plates were photographed after 7 d at 16°C and after 3 d at 30 or 37°C. (*C*) Benomyl partially suppresses the temperature sensitivity of *kip3*(ts) *dyn1Δ* and *kip3*(ts) *kar3Δ* strains. Strains wild-type (DS138), *kip3Δ* (DS613), *dynΔ* (DS749), *kip3-20*(ts) *dyn1Δ* (DS765), *kar3Δ102* (DS750), and *kip3-30*(ts) *kar3Δ* (DS752) were incubated at 23°C for 2 d in liquid YPD medium. Approximately 10^4 cells were spotted on solid YPD medium containing 1% DMSO and benomyl at the indicated concentration, and photographed after 3 d of growth at the indicated temperature. (*D*) *KIP3* and *KAR3* differ in their genetic interactions with *KIP1* and *CIN8*. Strains *kip1Δ cin8-101* (DS49), wild-type (DS141), *kar3Δ* (DS276), *kip3Δ* (DS614), *kar3Δ kip1Δ cin8-101* (DS689), and *kip3Δ kip1Δ cin8-101* (DS737) were incubated for 2 d at 23°C in YPD medium. Approximately 5×10^4 cells were spotted on YPD medium and incubated for 4 d at the indicated temperature. *kar3Δ* remediates the temperature-sensitive spindle assembly defect of the *cin8-101 kip1Δ* double mutant, whereas *kip3Δ* does not.

by both *kip3* and *dyn1* mutants may reflect a common function in insertion of the anaphase nucleus through the bud neck. Alternatively, the cumulative effect caused by loss of the sequential migration and insertion steps of nuclear migration may be greater than that caused by loss of migration or insertion individually. Similarly, *KIP3* could overlap with any of the other kinesin-related genes to perform an essential function, and this overlap would only result in a phenotype upon loss of both activities.

We tested for synthetic phenotypes by constructing double deletion mutants in the presence of a plasmid-based copy of one wild-type gene and then determined whether the strain remained viable after plasmid segregation (see Materials and Methods). The *kip3 dyn1*, *kip3 kar3*, and *kar3 dyn1* strains all required a complementing plasmid for viability (Fig. 8 *A*), indicating that these combinations were synthetically lethal. The *kip3 kip1*, *kip3 cin8*, *kip3 smy1*, and *kip3 kip2* double mutants were all viable and formed colonies equal in size to the single mutants at 16, 23, 30, and 37°C (at 37°C the *cin8* and *kip3 cin8* strains showed equally poor growth), indicating that these pairs of genes are not solely responsible for an essential function.

Simultaneous Loss of KIP3 and Dynein Function Causes Lethality but Does Not Abolish Any Specific Stage of Nuclear Migration

To distinguish whether *kip3* and *dyn1* mutations are synthetically lethal because of a functional overlap or due to a cumulative effect caused by partial loss of sequential functions, we examined a conditional double mutant. Temperature-sensitive *kip3*(ts) *dyn1Δ* strains were constructed by the plasmid shuffle technique (Fig. 8 *B*). A culture of the *kip3-20*(ts) *dyn1Δ* strain grown at 23°C contained 48% inviable cells, while *kip3Δ* and *dyn1Δ* single mutant cultures contained 95–100% viable cells. Incubation of the double mutant at 37°C for 4 h resulted in a doubling of cell number and a reduction of cell viability to 25%. Continued incubation at 37°C resulted in a second doubling of cell number by 16 h, at which time cell number ceased to increase and cell viability remained at 25%. This suggests that the synthetic lethality is not solely due to induction of a checkpoint that arrests cell cycle progression and prevents inviability.

Preanaphase nuclear migration was examined by microscopy of the double mutants after incubation at the nonpermissive temperature. The position of undivided nuclei was significantly more random in the *kip3*(ts) *dyn1Δ* double mutant than in the *dyn1* single mutant and wild-type strains (Fig. 4). However, the variance of the *kip3*(ts) *dyn1Δ* double mutant was not significantly different from the *kip3Δ* single mutant. This indicates that combination of *dyn1Δ* and *kip3*(ts) mutations causes no greater defect in nuclear migration to the neck than that caused by the *kip3Δ* mutation alone.

Both *kip3* and *dyn1* mutations individually cause a small delay in the nuclear division cycle before anaphase (see above and Yeh et al., 1995). The combination of *kip3*(ts) *dyn1Δ* mutations also caused a delay in the nuclear division cycle, which we observed as an increased frequency of preanaphase cells whose buds had grown beyond the size at which nuclear division normally occurs. Double mutant cells incubated at 37°C for 4 h showed the delay at a frequency 2.5-fold higher than the *kip3* and *dyn1* single mutants and 10-fold higher than the wild-type strain (Table II). The *kip3*(ts) *dyn1* cells incubated at the nonpermissive temperature exhibited an abnormal morphology that was not observed in either single mutant. Mother cells and ma-

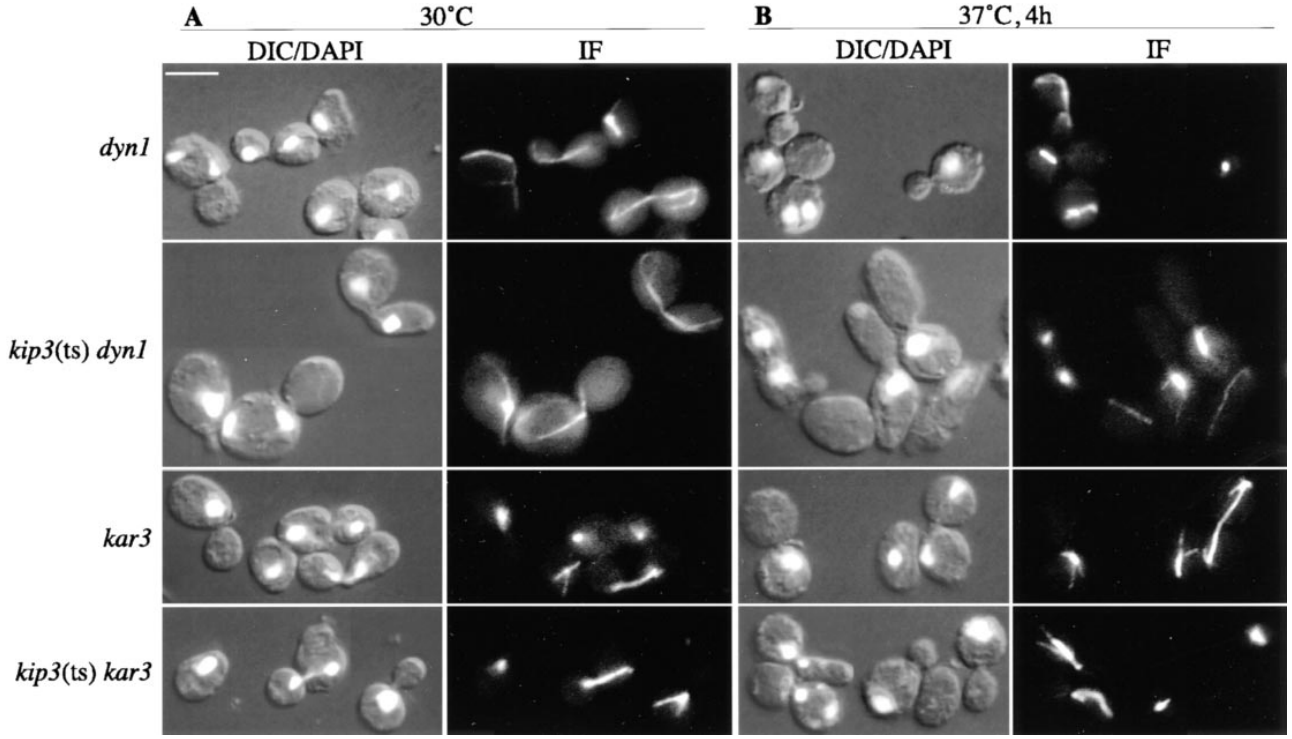

Figure 9. Morphology of *kip3 dyn1* and *kip3 kar3* double mutants. (*A*) The indicated strains were grown to mid-logarithmic phase at 30°C in YPD medium and fixed for microscopy. (*B*) The same cultures shifted to 37°C for 4 h. The columns labeled DIC/DAPI are DIC images overlaid with corresponding DAPI-stained images to show position of nuclear DNA, and the columns labeled IF are corresponding images of antitubulin staining to visualize microtubules. Binucleate mother cells are present in the *dyn1*, *kip3*(ts) *dyn1*, and *kip3*(ts) *kar3* mutants but not in the *kar3* mutant. The strain designations are the same as in Fig. 8. Bar, 5 μm.

ture buds were enlarged and elongated, but small buds had a normal ellipsoidal shape (Fig. 9). Abnormal cell elongation can be caused by mutations affecting a variety of functions (Blacketer et al., 1995), including defects in the switch from apical to isotropic growth that occurs at the G2/M transition (Lew and Reed, 1993).

To determine whether *KIP3* and *DYN1* overlap in function for insertion of the nucleus into the neck during anaphase spindle elongation, we measured the frequency of mother cells containing two discrete nuclear DNA masses. The *kip3*(ts) *dyn1* double mutant culture incubated at 37°C for 4 h contained 10% binucleate mother cells (Table II), compared to 6% binucleate cells in *kip3* and *dyn1* single mutants. An independent *kip3*(ts) allele in a *dyn1Δ* strain had a similar cell type distribution. Since the double mutant culture incubated for 4 h at 37°C still contained some anaphase cells, we examined a culture incubated for 8 h at 37°C and found that the binucleate mother cells increased to 23%. Thus, simultaneous loss of *KIP3* and *DYN1* function causes defective insertion of anaphase spindles through the bud neck, in addition to causing defective preanaphase nuclear migration and a metaphase delay. This suggests that the synthetic lethality of *kip3 dyn1* mutants is a cumulative effect caused by loss of partially overlapping and sequential functions.

Since one phenotype of the *kip3Δ* single mutant and the *kip3*(ts) *dyn1Δ* double mutant is increased microtubule abundance (Figs. 3 and 9), we tested whether the microtubule-depolymerizing drug benomyl could suppress the lethality of the *kip3*(ts) *dyn1Δ* double mutant. The double mutant showed little growth at 37°C in the absence of benomyl but exhibited significant growth on media containing 5 or 10 μg/ml benomyl (Fig. 8 *C*). This suggests that altered microtubule polymerization in the double mutant is a contributing factor to the synthetic lethality.

Simultaneous Loss of KIP3 and KAR3 Function Generates No Strong Synthetic Morphological Defect

The kinesin-related Kar3p is a candidate to provide some of the same functions as Kip3p because loss of either *KIP3* or *KAR3* causes increased astral microtubule abundance (above and Saunders et al., 1997), and Kar3p is known to mediate one nuclear movement, nuclear congression, during karyogamy (Meluh and Rose, 1990). To determine the nature of the defects caused by simultaneous loss of *KIP3* and *KAR3* function, the plasmid shuffle technique was used to isolate a temperature-conditional double mutant (Fig. 8 *B*). Like the *kip3*(ts) *dyn1* double mutant, lethality of the *kip3-30*(ts) *kar3Δ* double mutant was partially suppressed on medium containing a low concentration of benomyl (Fig. 8 *C*). To examine morphological defects, the *kip3*(ts) *kar3Δ* double mutant was incubated at the nonpermissive temperature, and the cells were compared to *kar3Δ* and *kip3Δ* single mutants by microscopy. The *kar3Δ* single mutant showed a high proportion of cells before anaphase (Table II), with many of the nuclei in very close proximity to the bud neck (Fig. 4), as previously re-

ported (Meluh and Rose, 1990). When the *kip3 kar3* double mutant was incubated at 37°C for 4 h, fewer nuclei were in very close proximity to the neck, and more were at the distal edge of the mother cell (Fig 4). This suggests that the migration defect caused by *kip3* mutation is epistatic to the accumulation of nuclei in very close proximity to the bud caused by *kar3* mutation. No other aberrant morphology unique to the double mutant was detected (Fig. 9). The data in Table II show that the frequency of cells in metaphase in the *kip3 kar3* double mutant culture was similar to that in *kar3* single mutant, and the frequency of binucleate cells was similar to that in the *kip3* single mutant. Thus, the combination of *kip3* and *kar3* mutations caused the aberrant morphologies characteristic of the individual mutations to be superimposed and did not result in a detectable synthetic morphological phenotype.

KIP3 and KAR3 Differ in Their Genetic Interactions with KIP1 and CIN8

Given the possibility of functional overlap suggested by the synthetic lethality of *kip3* and *kar3*, we examined whether Kip3p could perform a previously described function of Kar3p in contributing to the balance of inwardly and outwardly acting forces that maintain mitotic spindle pole separation during metaphase. Mutations in kinesin-related genes *KIP1* and *CIN8* can cause collapse of the metaphase spindle, suggesting that Kip1p and Cin8p act to maintain spindle pole separation, and mutations in *KAR3* can suppress this collapse phenotype and restore growth, suggesting that Kar3p generates an inward force on the spindle poles (Saunders and Hoyt, 1992; Hoyt et al., 1993). Mutations in *KAR3* may suppress the *kip1 cin8* collapse phenotype by stabilizing microtubules, and a mutation in the β-tubulin gene that stabilizes microtubules has an effect similar to *kar3* mutation (Saunders et al., 1997). To determine whether Kip3p can perform a role similar to Kar3p in countering the forces generated by Kip1p and Cin8p, we tested whether a *kip3Δ* mutation can suppress the *kip1 cin8* growth defect. Meiotic crosses were used to construct *kip3 kip1 cin8* and *kar3 kip1 cin8* triple mutants, and the sensitivity of growth to temperature was examined (Fig. 8 *D*). The *kar3Δ* mutation partially suppressed the temperature-sensitive growth of the *kip1 cin8* mutant as expected, but the *kip3Δ* mutation did not. Thus, *KIP3* fails to show genetic interactions with *KIP1* and *CIN8*, indicating that Kip3 does not overlap with the suggested role of Kar3p in generating an inwardly directed spindle force, and further suggests that Kip3p and Kar3p perform separate functions.

Kip3p is Present on Both Astral and Central Spindle Microtubules

The phenotypes of the *kip3Δ* mutant suggested roles for Kip3p primarily in astral microtubule function. To determine if Kip3p is associated with microtubules in vivo, we determined the intracellular localization of a functional epitope-tagged protein. A single-copy plasmid expressing myc-tagged Kip3p (*KIP3-6MYC*, see Materials and Methods) from its own promoter was introduced into a *kip3Δ* strain. Western blotting of an extract from this strain identified a single band at the predicted molecular mass of 100 kD (data not shown). In G1 cells, Kip3p colocalized with the astral microtubules (Fig. 10, *A–C*). In late S phase or early mitotic cells, Kip3p colocalized with short bipolar spindles (Fig. 10, *D–F*). In late anaphase or telophase cells, Kip3p colocalized with spindle microtubules and was frequently concentrated near the spindle midzone, the zone of overlap between microtubules from opposite poles (65% of late mitotic cells where Kip3p spindle localization was observed, $n = 250$; Fig.10, *G–I*). In the remaining late mitotic cells, Kip3p staining was evenly distributed along the length of the elongated spindle (Fig. 10, *J–L*). In addition to microtubule staining, expression of *KIP3-6MYC* resulted in bright punctate staining of the nucleus and cytoplasm of all cells observed. This punctate staining was not observed over the vacuole and was specific to Kip3p-6myc because it was not observed in an untagged *KIP3* control strain (Fig. 10, *M–O*). We were able to detect microtubule localization of Kip3p in 11% of the cells examined ($n = 300$). It is possible that microtubule staining in many cells was obscured by the generalized staining.

Discussion

The Complete Set of S. cerevisiae Kinesin–related Proteins

A search of the complete yeast genome sequence revealed *KIP3* as the single previously uncharacterized gene encoding a protein with strong sequence conservation with the force-generating domain of kinesin. Thus, budding yeast contains six genes encoding kinesin-related proteins (*KIP1, KIP2, KIP3, KAR3, CIN8*, and *SMY1*), and it is the first organism whose complete set of kinesin-related proteins has been identified. Three of the kinesin-related proteins are members of known kinesin subfamilies defined by sequence conservation; *KIP1* and *CIN8* belong to the BimC subfamily and *KAR3* belongs to the COOH-terminal subfamily (Moore and Endow, 1996). Members of these two subfamilies show functional conservation as well as sequence conservation, with members of the BimC subfamily playing roles in mitotic spindle assembly and members of the COOH-terminal subfamily playing roles in spindle pole function. The kinesin-related proteins encoded by *KIP2, KIP3*, and *SMY1* lack any strong subfamily homology.

The relatively small number of microtubule-mediated movements that occur in yeast can now be ascribed to the force generated by the six kinesins, dynein, and potentially to forces generated by microtubule polymerization and depolymerization. No single motor protein is essential for viability, perhaps because of cooperation between different force-generating mechanisms, such as the overlap between *KIP1* and *CIN8* for mitotic spindle assembly (Hoyt et al., 1992; Roof et al., 1992). Given the complete set of motor proteins, it is now possible to systematically dissect the contribution of each motor protein to a particular microtubule-based movement.

A Kinesin-related Protein Required for Nuclear Migration

We used two experimental approaches to characterize the

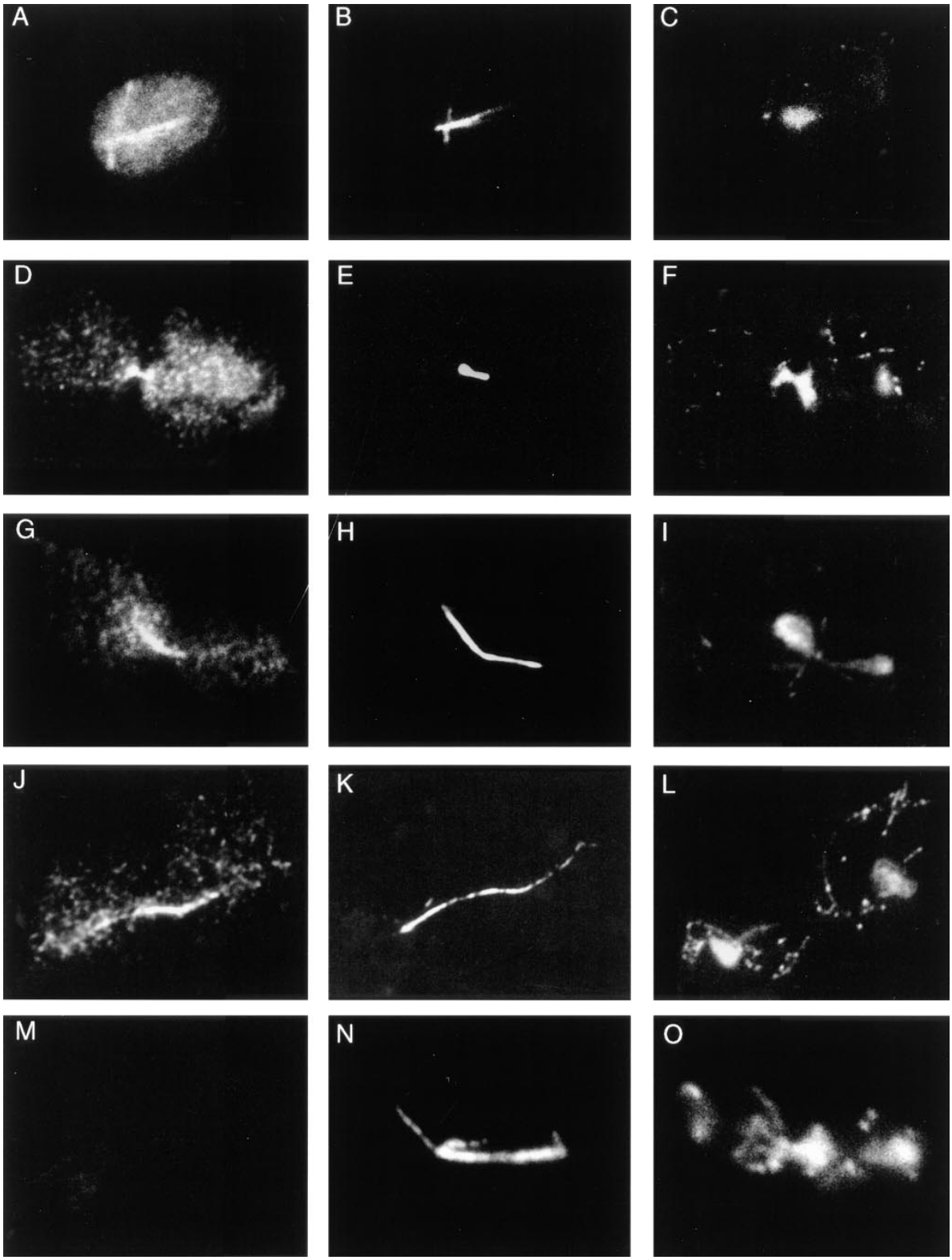

Figure 10. Epitope-tagged Kip3p localizes to astral and spindle microtubules and is present in the cytoplasm and nucleoplasm. The cells are from an asynchronous culture containing epitope-tagged Kip3p expressed from a centromere plasmid. The first column (*A*, *D*, *G*, *J*, and *M*) shows staining with 9E10, an anti-myc antibody that recognizes epitope-tagged Kip3p. The second column (*B*, *E*, *H*, *K*, and *N*) shows staining with an antitubulin antibody. The third column (*C*, *F*, *I*, *L*, and *O*) shows staining with DAPI to localize DNA. (*A–C*) A G1 cell with colocalization of Kip3p with astral microtubules. (*D–F*) A preanaphase cell with spindle staining. (*G–L*) Cells with an elongated anaphase spindle with concentration of Kip3p in the central spindle. (*M–O*) A cell of an isogenic strain carrying Kip3p lacking the epitope tag, which showed no signal when stained and photographed under conditions identical to those used to localize epitope-tagged Kip3p.

effect of loss of *KIP3* function on nuclear migration. In the first approach, we examined populations of fixed cells to assess the position of the nucleus and orientation of the mitotic spindle relative to the bud. Undivided nuclei in budded wild-type cells had a strong tendency to be located ~1 μm from the neck, and the associated mitotic spindle had a strong tendency to be oriented within 30 degrees of the mother–daughter axis, consistent with previous studies of *S. cerevisiae* morphology (Byers and Goetsch, 1975; Jacobs et al., 1988). Both position and orientation of the nucleus became essentially random upon loss of *KIP3* function. Since these experiments relied on use of the bud as a reference point to quantitate the position and orientation of undivided nuclei, they define an essential role for *KIP3* for directed nuclear migration and orientation during the cell cycle interval from Start to just before anaphase. We were unable to use fixed cells to quantitate nuclear movements in G1 phase cells because these cells lack a bud to use as a reference point.

In the second experimental approach to characterize nuclear migration, we used live cell microscopy to follow movement of the spindle pole body in individual cells. In addition to defining the path and kinetics of movement during nuclear migration, this approach enabled us to examine nuclear positioning during the G1 phase of the cell cycle. By observing nuclear migration in a live cell through the point of bud emergence, we could infer the site of bud emergence for use as a reference point in G1 phase cells. Bud emergence in haploid cells follows the axial pattern of bud site selection, in which the new bud emerges adjacent to the previous division site (Chant and Pringle, 1995). A consequence of axial budding is that anaphase spindle elongation places the nucleus at the edge of the cell opposite to the site of bud emergence.

The first spindle-independent movement of the nucleus occurs immediately after spindle disassembly, when the nucleus rapidly moves toward the cell center (Fig. 6 and Yeh et. al., 1995). We observed this movement in wild-type, *kip3*, and *dyn1* strains. In the subsequent period of movement, the nucleus continued toward the prebud site, with steady forward movement and no large reversals in direction. The second period of movement sometimes occurred immediately after the initial movement, so that migration was complete within 15 min of spindle disassembly, before a bud could be seen. In other examples, there was a delay of about 20 min before the second period of movement occurred. The new bud can be detected only at the end of G1, but actin, Spa2p, and neck filament proteins localize to the prebud site before bud emergence (Kim et al., 1991; Snyder et al., 1991; Lew and Reed, 1993). Although there are differences in the reported timing of assembly of proteins at the prebud site, the intersection of astral microtubules with the prebud site provide a potential mechanism for directed nuclear migration during G1. When the nucleus reached a site ~1 μm from the bud neck, its position became relatively stable. We observed similar patterns of preanaphase movement in wild-type and *dyn1* strains.

Loss of *KIP3* function caused a dramatically different course of phase 1 nuclear migration. After the *kip3* mutant completed the rapid inward movement after spindle disassembly, nuclei exhibited large forward and reverse oscillations in position relative to the bud neck (see Fig. 6, *C* and *D*). The nucleus sometimes came within ~1 μm of the neck, only to reverse direction and move 1–2 μm in the opposite direction. Since the nuclei were located far from the neck for long time intervals, the oscillations are consistent with the random position of nuclei observed in populations of fixed *kip3* cells. Furthermore, the oscillations may account for the viability of mutants lacking *KIP3* function because nuclei are occasionally at the "correct" location ~1 μm from the neck.

Distinct Steps of Nuclear Migration Defined by Mutations in KIP3 and DYN1

Nuclear migration is a pathway comprised of a series of distinct movements that occur during interphase and mitosis. We found that mutations in *KIP3* predominantly affected the first phase of nuclear migration as the undivided nucleus moved to a site ~1 μm from the neck, and the metaphase spindle oriented along the mother–daughter axis (Fig. 11, *Phase 1*). In contrast, the *dynΔ* mutation predominantly affected the second phase of nuclear migration as the spindle began to elongate during anaphase, and the nucleus inserted into the neck, consistent with the previous detailed analysis of nuclear movement by Yeh et al. (1995). We detected only a small effect of *kip3* mutation on the second phase of nuclear migration, and little effect of *dyn1* mutation on the first phase of nuclear migration. Thus, the phenotypes of mutants singly defective in *KIP3* and *DYN1* fell into two classes that define distinct steps in the nuclear migration pathway.

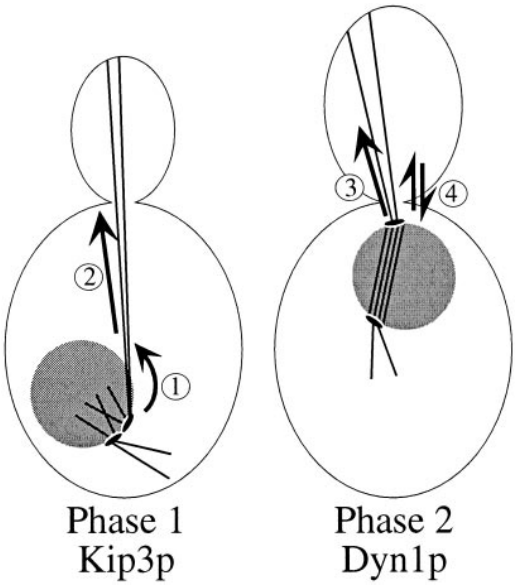

Figure 11. Distinct roles of Kip3p and Dyn1p in the two phases of nuclear migration. Based on the phenotypes of *kip3* and *dyn1* mutants, Kip3p primarily functions during phase 1 of nuclear migration to (*1*) orient the nucleus toward the nascent bud and (*2*) position the nucleus ~1 μm from the bud neck. During phase 2 of nuclear migration, Dyn1p primarily functions to (*3*) insert the anaphase-stage nucleus through the neck and (*4*) mediate forward and reverse oscillations of the nucleus within the neck.

The nuclear migration defects of *dyn1* mutants during anaphase support the hypothesis that dynein is part of the force-generating machinery that squeezes the nucleus through the narrow neck opening. However, we found very little effect of loss of dynein function on nuclear position or spindle orientation from the time of cytokinesis to anaphase initiation. This is in contrast to *Aspergillus nidulans* and *Neurospora crassa*, where dynein is required after nuclear division for migration of nuclei into the mycelium (Plamann et al., 1994; Xiang et al., 1994). Our results do not contradict most previous reports of incorrect spindle orientation in *S. cerevisiae* mutants lacking dynein or dynactin function because these studies examined the orientation of anaphase spindles in binucleate mother cells and did not address nuclear position or spindle orientation in preanaphase cells (Eshel et al., 1993; Li et al., 1993; McMillan and Tatchell, 1994; Muhua et al., 1994). However, Yeh et al. (1995) suggest that orientation of the spindle as the nucleus contacts the neck during early anaphase is defective in *dyn1* mutants. We have not examined spindle orientation as anaphase initiates in an unbiased set of *kip3* or *dyn1* cells and do not rule out a possible role for dynein in spindle orientation as the elongating anaphase nucleus docks onto the neck. The absence of a detectable effect of dynein mutation on interphase nuclear migration may be explained by functional overlap between dynein and other force-generating mechanisms.

Mutants defective in *KIP3* or *DYN1* have one phenotype in common: the generation of mother cells that contain two nuclei connected by a spindle that is frequently not aligned along the mother–daughter axis. Our analysis of *dyn1* mutants suggests that binucleate cells in this mutant may arise not because of spindle misorientation, but instead because of failed translocation of the anaphase-stage nucleus through the neck. However, formation of binucleate mother cells upon loss of *KIP3* function may be caused by a defect in an independent mechanism. The defects of *kip3* mutants in phase 1 nuclear migration suggest that binucleate cells could be formed when anaphase is initiated while the nucleus is improperly located or oriented. The mechanism by which binucleate mother cells arise in *kip3* and *dyn1* mutants could be addressed more directly by observing nuclear position and spindle orientation during anaphase initiation when a binucleate mother cell is formed, but we have been unable to record such an event in either *kip3* or *dyn1* strains by microscopy of individual live cells. Mutations in many other *S. cerevisiae* genes cause binucleate mother cells to accumulate (for review see Morris et al., 1995). It would be interesting to use the approaches described here to test whether these mutations affect the first or second phase of the nuclear migration pathway.

A model for how Kip3p controls nuclear movement and orientation should take into account the observations that the *kip3* mutant exhibits large oscillations of nuclear position and has higher resistance to the microtubule-depolymerizing drug benomyl than to wild-type strains. Both of these phenotypes could be the result of altered microtubule dynamics. One explanation for the benomyl resistance is that microtubules are more stable because loss of *KIP3* function eliminates a microtubule depolymerizing activity. Destabilization of microtubules by kinesin-related proteins has been described for Kar3p at the minus ends of microtubules and for *Xenopus* XKCM1 protein at the plus ends, and altered astral microtubule dynamics occur in *S. cerevisiae* mutants lacking dynein (Endow et al., 1994; Walczak et al., 1996; Carminati and Stearns, 1997). Although Kip3p and Kar3p may both affect microtubule dynamics, these proteins differ in that Kar3p is concentrated at the spindle poles (Saunders et al., 1997), and Kip3p is located throughout the cytoplasm and nucleus and is present on both astral and spindle microtubules. Furthermore, loss of *KAR3* function has a different effect on the balance of forces in the mitotic spindle perturbed by *kip1* and *cin8* mutation than does loss of *KIP3*.

One model for Kip3p function is that Kip3p interacts with the plus ends of microtubules, enabling it to control astral microtubule dynamics and thereby influence the forces applied to the nucleus. In the absence of Kip3p, the positional oscillations of preanaphase nuclei could be powered by unregulated polymerization and depolymerization of the astral microtubules that extend into the bud and terminate near the cortex. Other motor proteins could also power the positional oscillations, but the morphology of *kip3 dyn1* and *kip3 kar3* double mutants suggests that Dyn1p or Kar3p are not individually responsible for powering the nuclear oscillations (see below). In addition to regulating microtubule dynamics, Kip3p may directly generate the force applied to the nucleus for nuclear migration. The wide distribution of Kip3p in the cell suggests that astral microtubules interact with Kip3p either transiently, or with a specific subpopulation of Kip3p. One possibility is that a subpopulation of Kip3p is attached to an asymmetrically distributed cortical protein such as Num1p or proteins located at the prebud site (Snyder et al., 1991; Farkasovsky and Kuntzel, 1995; Pringle et al., 1995), and that these Kip3p molecules push or pull the nucleus toward the bud neck.

Synthetic Lethality and Functional Overlap

While mutants individually defective in *KIP3* or *DYN1* defined distinct steps of nuclear migration, these proteins could perform additional roles that are not evident in the single mutants because of functional overlap among different force generating mechanisms. We explored this possibility by testing for synthetic lethality between the *kip3Δ* mutation and mutations in the *DYN1* gene and each of the kinesin-related genes, and we found that *kip3* is synthetically lethal with *dyn1* and *kar3*. However, in the W303-1a strain background, we could recover very slow-growing but viable *kip3Δ dyn1Δ* double mutants (data not shown). To determine whether the synthetic lethality was due to the loss of a single essential movement, we constructed conditional double mutants and examined cell and microtubule morphology. In both the *kip3 dyn1* and *kip3 kar3* conditional double mutants, there was no accumulation of a structural intermediate in nuclear migration or mitosis that suggested that a specific movement was abolished. The *kip3 dyn1* conditional double mutant culture contained cells delayed in metaphase at a frequency 2.5 times that observed in the single mutants, and there was a higher frequency of cells with two separate DNA masses in the mother cell than in either single mutant (a fourfold in-

crease). However, the binucleate mother cells may arise as a consequence of separate defects. Preanaphase nuclear positioning was essentially random in both the *kip3* single mutant and in the *kip3 dyn1* double mutant. Since no single detectable defect in the *kip3 dyn1* double mutant appears to account for the synthetic lethality, we suspect that the synthetic lethality is caused by the cumulative effect of partial defects in sequential movements. Synthetic lethality due to partial loss of sequentially acting functions has been described (Simon et al., 1991). A similar conclusion is suggested by the morphology of the *kip3 kar3* conditional double mutant, which essentially exhibits a superimposition of the defects observed in the single mutants. However, we cannot rule out the possibility that Kip3p and Dyn1p or Kip3p and Kar3p overlap to perform a movement or function whose loss does not generate a detectable morphological defect. Furthermore, the localization of Kip3p to central spindle microtubules suggests that our analysis has not revealed the full functional repertoire of Kip3p.

Kinesin-related Proteins and Nuclear Migration

Nuclear positioning and spindle orientation are key regulated steps of cell growth and development in many organisms. Nuclear migration plays an important role for fertilization in higher cells and in yeast for the analogous process of karyogamy (Meluh and Rose, 1990; Rouviere et al., 1994). Nuclear migration is also central to development. In *Caenorhabditis elegans*, asymmetric positioning of the nucleus during the first cell division of the zygote results in the production of daughter cells that differ in size and developmental fate (Hyman and White, 1987). During the syncytial stage of development in *Drosophila*, nuclear migration determines the position of both the germ cells and the somatic cells (Baker et al., 1993). Also in *Drosophila*, patterned changes in spindle orientation mediate developmental fate in the parts of the nervous system (Kraut et al., 1996).

Although it is thought that both the tubulin and actin cytoskeletons are important for nuclear migration, few of the force-generating molecules required for nonmitotic nuclear movement have been identified. The *S. cerevisiae* kinesin–related protein Kar3p is essential for karyogamy (Meluh and Rose, 1990), and *A. nidulans* and *N. crassa* cytoplasmic dynein is required for movement of nuclei in the germ tube (Plamann et al., 1994; Xiang et al., 1994). In this study, we found that another yeast kinesin–related protein, Kip3p, plays a critical role in spindle orientation and nuclear position before anaphase. Kinesin-related proteins may therefore have a general role in nuclear migration. Furthermore, because kinesin-related proteins are found in all eukaryotes, these motors might also control developmentally regulated nuclear movement in multicellular organisms.

The authors would like to thank J. Kahana and P. Silver for the *NUF2–GFP* plasmid, E. Yeh and K. Bloom for the *dynΔ* plasmid, J. Carminati and T. Stearns for sharing unpublished results, and D. Gordon, B. Bucher, and T. Yen for comments on the manuscript.

This work was supported by grants from the National Institutes of Health (R55-GM50884) and the University of Pennsylvania Research Foundation to D. Roof. D. Pellman is supported by a Damon Runyon Scholar Award, and T. DeZwaan was supported by a training grant from the National Institutes of Health (GM07229).

Received for publication 19 May 1997 and in revised form 3 July 1997.

References

Baker, J., W.E. Theurkauf, and G. Schubiger. 1993. Dynamic changes in microtubule configuration correlate with nuclear migration in the preblastoderm *Drosophila* embryo. *J. Cell Biol.* 122:113–121.

Baudin, A., O. Ozier-Kalogeropoulos, A. Denouel, F. Lacroute, and C. Cullin. 1993. A simple and efficient method for direct gene deletion in *Saccharomyces cerevisiae. Nucleic Acids Res.* 21:3329–3330.

Blacketer, M.J., P. Madaule, and A.M. Myers. 1995. Mutational analysis of morphologic differentiation in *Saccharomyces cerevisiae. Genetics.* 140: 1259–1275.

Boeke, J.D., J. Trueheart, G. Natsoulis, and G.R. Fink. 1987. 5-Fluoro-orotic acid as a selective agent in yeast molecular genetics. *Methods Enzymol.* 154: 164–175.

Byers, B., and L. Goetsch. 1975. Behavior of spindles and spindle plaques in the cell cycle and conjugation in *Saccharomyces cerevisiae. J. Bacteriol.* 124:511.

Carminati, J.L., and T. Stearns. 1997. Microtubules orient the mitotic spindle in yeast through dynein-dependent interactions with the cell cortex. *J. Cell Biol.* 138:629–641.

Chant, J., and J.R. Pringle. 1995. Patterns of bud-site selection in the yeast *Saccharomyces cerevisiae. J. Cell Biol.* 129:751–765.

Conde, J., and G.R. Fink. 1976. A mutant of *Saccharomyces cerevisiae* defective for nuclear fusion. *Proc. Natl. Acad. Sci. USA.* 73:3651–3655.

Endow, S.A., S.J. Kang, L.L. Satterwhite, M.D. Rose, V.P. Skeen, and E.D. Salmon. 1994. Yeast Kar3 is a minus-end microtubule motor protein that destabilizes microtubules preferentially at the minus ends. *EMBO (Eur. Mol. Biol. Organ.) J.* 13:2708–2713.

Eshel, D., L.A. Urrestarazu, S. Vissers, J.-C. Jauniaux, J.C. van Vliet-Reedijk, R.J. Planta, and I.R. Gibbons. 1993. Cytoplasmic dynein is required for normal nuclear segregation in yeast. *Proc. Natl. Acad. Sci. USA.* 90:11172–11176.

Evan, G.I., G.K. Lewis, G. Ramsay, and J.M. Bishop. 1985. Isolation of monoclonal antibodies specific for human c-myc proto-oncogene product. *Mol. Cell. Biol.* 5:3610–3616.

Farkasovsky, M., and H. Kuntzel. 1995. Yeast Num1p associates with the mother cell cortex during S/G2 phase and affects microtubular functions. *J. Cell Biol.* 131:1003–1014.

Hoyt, M.A., L. He, K.K. Loo, and W.S. Saunders. 1992. Two *Saccharomyces cerevisiae* kinesin-related gene products required for mitotic spindle assembly. *J. Cell Biol.* 118:109–120.

Hoyt, M.A., L. He, L. Totis, and W.S. Saunders. 1993. Loss of function of *Saccharomyces cerevisiae* kinesin-related *CIN8* and *KIP1* is suppressed by *KAR3* motor domain mutations. *Genetics.* 135:35–44.

Huffaker, T.C., J.H. Thomas, and D. Botstein. 1988. Diverse effects of β-tubulin mutations on microtubule formation and function. *J. Cell Biol.* 106:1997–2010.

Hyman, A.A., and J.G. White. 1987. Determination of cell division axes in the early embryogenesis of *Caenorhabditis elegans. J. Cell Biol.* 105:2123–2135.

Jacobs, C.W., A.E.M. Adams, P.J. Szaniszlo, and J.R. Pringle. 1988. Functions of microtubules in the *Saccharomyces cerevisiae* cell cycle. *J. Cell Biol.* 107: 1409–1426.

Kahana, J.A., B.J. Schnapp, and P.A. Silver. 1995. Kinetics of spindle pole body separation in budding yeast. *Proc. Natl. Acad. Sci. USA.* 92:9707–9711.

Kim, H.B., B.K. Haarer, and J.R. Pringle. 1991. Cellular morphogenesis in the *Saccharomyces cerevisiae* cell cycle: localization of the CDC3 gene product and the timing of events at the budding site. *J. Cell Biol.* 112:535–544.

Kraut, R., W. Chia, L.Y. Jan, Y.N. Jan, and J.A. Knoblich. 1996. Role of inscuteable in orienting asymmetric cell divisions in *Drosophila. Nature (Lond.).* 383:50–55.

Lew, D.J., and S.I. Reed. 1993. Morphogenesis in the yeast cell cycle: regulation by Cdc28 and cyclins. *J. Cell Biol.* 120:1305–1320.

Li, R. 1997. Bee1, a yeast protein with homology to Wiscott-Aldrich syndrome protein, is critical for the assembly of cortical actin cytoskeleton. *J. Cell Biol.* 136:649–658.

Li, Y., E. Yeh, T. Hays, and K. Bloom. 1993. Disruption of mitotic spindle orientation in a yeast dynein mutant. *Proc. Natl. Acad. Sci. USA.* 90:10096–10100.

Lupas, A., M.V. Dyke, and J. Stock. 1991. Predicting coiled coils from protein sequences. *Science (Wash. DC).* 252:1162–1164.

McMillan, J.N., and K. Tatchell. 1994. The *JNM1* gene in the yeast *Saccharomyces cerevisiae* is required for nuclear migration and spindle orientation during the mitotic cell cycle. *J. Cell Biol.* 125:143–158.

Meluh, P.B., and M.D. Rose. 1990. *KAR3*, a kinesin-related gene required for yeast nuclear fusion. *Cell.* 60:1029–1041.

Moore, J.D., and S.A. Endow. 1996. Kinesin proteins: a phylum of motors for microtubule-based motility. *BioEssays.* 18:207–219.

Morris, N.R., X. Xiang, and S.M. Beckwith. 1995. Nuclear migration advances in fungi. *Trends Cell Biol.* 5:278–282.

Muhua, L., T.S. Karpova, and J.A. Cooper. 1994. A yeast actin-related protein

homologous to that in vertebrate dynactin complex is important for spindle orientation and nuclear migration. *Cell.* 78:669–679.

Navone, F., J. Niclas, N. Hom-Booher, L. Sparks, H.D. Bernstein, G. McCaffrey, and R.D. Vale. 1992. Cloning and expression of a human kinesin heavy chain gene: interaction of the COOH-terminal domain with cytoplasmic microtubules in transfected CV-1 cells. *J. Cell Biol.* 117:1263–1275.

Palmer, R.E., M. Koval, and D. Koshland. 1989. The dynamics of chromosome movement in the budding yeast *Saccharomyces cerevisiae. J. Cell Biol.* 109: 3355.

Palmer, R.E., D.S. Sullivan, T. Huffaker, and D. Koshland. 1992. Role of astral microtubules and actin in spindle organization and migration in the budding yeast, *Saccharomyces cerevisiae. J. Cell Biol.* 119:583–593.

Pellman, D., M. Bagget, H. Tu, and G.R. Fink. 1995. Two microtubule-associated proteins required for anaphase spindle movement in *Saccharomyces cerevisiae. J. Cell Biol.* 130:1373–1385.

Plamann, M., P.F. Minke, J.H. Tinsley, and K.S. Bruno. 1994. Cytoplasmic dynein and actin-related protein Arp1 are required for normal nuclear distribution of filamentous fungi. *J. Cell Biol.* 127:139–149.

Pringle, J.R., E. Bi, H.A. Hardins, J.E. Zahner, C. De Virgilio, J. Chant, K. Corrado, and H. Fares. 1995. Establishment of cell polarity in yeast. *Cold Spring Harbor Symp. Quant. Biol.* 60:729–744.

Roof, D.M., P.B. Meluh, and M.D. Rose. 1992. Kinesin-related proteins required for assembly of the mitotic spindle. *J. Cell Biol.* 118:95–108.

Rose, M.D., and G.R. Fink. 1987. *KAR1*, a gene required for function of both intranuclear and extranuclear microtubules in yeast. *Cell.* 48:1047–1060.

Rose, M.D., F. Winston, and P. Hieter. 1990. Methods in Yeast Genetics. Cold Spring Harbor Laboratory Press, Cold Spring Harbor, NY. 198 pp.

Rothstein, R.J. 1983. One-step gene disruption in yeast. *Methods Enzymol.* 101: 202–211.

Rouviere, C., E. Houliston, D. Carre, P. Chang, and C. Sardet. 1994. Characteristics of pronuclear migration in *Beroe ovata. Cell Motil. Cytoskel.* 29:301–311.

Saunders, W., D. Hornack, V. Lengyel, and C. Deng. 1997. The *Saccharomyces cerevisiae* kinesin-related motor Kar3p acts at preanaphase spindle poles to limit the number and length of cytoplasmic microtubules. *J. Cell Biol.* 137: 417–431.

Saunders, W.S., and M.A. Hoyt. 1992. Kinesin-related proteins required for structural integrity of the mitotic spindle. *Cell.* 70:451–459.

Saunders, W.S., D. Koshland, D. Eshel, I.R. Gibbons, and M.A. Hoyt. 1995. *Saccharomyces cerevisiae* kinesin- and dynein-related proteins required for anaphase chromosome segregation. *J. Cell Biol.* 128:617–624.

Sikorski, R.S., and P. Hieter. 1989. A system of shuttle vectors and yeast host strains designed for efficient manipulation of DNA in *Saccharomyces cerevisiae. Genetics.* 122:19–27.

Simon, M.A., D.D. Bowtell, G.S. Dodson, T.R. Laverty, and G.M. Rubin. 1991. Ras1 and a putative guanine nucleotide exchange factor perform crucial steps in signaling by the sevenless protein tyrosine kinase. *Cell.* 67:701–716.

Snyder, M., S. Gehrung, and B.D. Page. 1991. Studies concerning the temporal and genetic control of cell polarity in *Saccharomyces cerevisiae. J. Cell Biol.* 114:515–532.

Spencer, F., S.L. Gerring, C. Connelly, and P. Hieter. 1990. Mitotic chromosome transmission fidelity mutants in *Saccharomyces cerevisiae. Genetics.* 124:237–249.

Stearns, T., M.A. Hoyt, and D. Botstein. 1990. Yeast mutants sensitive to antimicrotubule drugs define three genes that affect microtubule function. *Genetics.* 124:251–262.

Sullivan, D.S., and T.C. Huffaker. 1992. Astral microtubules are not required for anaphase B in *Saccharomyces cerevisiae. J. Cell Biol.* 119:379–388.

Walczak, C.E., T.J. Mitchison, and A. Desai. 1996. XKCM1: a *Xenopus* kinesin-related protein that regulates microtubule dynamics during mitotic spindle assembly. *Cell.* 84:37–47.

Xiang, X., S.M. Beckwith, and N.R. Morris. 1994. Cytoplasmic dynein is involved in nuclear migration in *Aspergillus nidulans. Proc. Natl. Acad. Sci. USA.* 91:2100–2104.

Yang, S.S., E. Yeh, E.D. Salmon, and K. Bloom. 1997. Identification of a mid-anaphase checkpoint in budding yeast. *J. Cell Biol.* 136:345–354.

Yeh, E., R.V. Skibbens, J.W. Cheng, E.D. Salmon, and K. Bloom. 1995. Spindle dynamics and cell cycle regulation of dynein in the budding yeast, *Saccharomyces cerevisiae. J. Cell Biol.* 130:687–700.